

1 Adaptive emission reduction approach to reach 2 any global warming target

3

4 **Jens Terhaar^{1,2*}, Thomas L. Frölicher^{1,2}, Mathias T. Aschwanden^{1,2}, Pierre Friedlingstein^{3,4}, Fortunat
5 Joos^{1,2}**

6 ¹ Climate and Environmental Physics, Physics Institute, University of Bern, Switzerland

7 ² Oeschger Centre for Climate Change Research, University of Bern, Switzerland

8 ³ College of Engineering, Mathematics and Physical Sciences, University of Exeter, Exeter EX4 4QF, UK

9 ⁴ Laboratoire de Météorologie Dynamique, Institut Pierre-Simon Laplace, CNRS-ENS-UPMC-X, Paris,
10 France

11

12

13 ***Jens Terhaar**

14 **Climate and Environmental Physics, Physics Institute**

15 **University of Bern**

16 **Sidlerstrasse 5**

17 **3012 Bern**

18 **Switzerland**

19 **jens.terhaar@unibe.ch**

20 The parties of the Paris Agreement agreed to keep global warming well below 2°C and pursue efforts to
21 limit it to 1.5°C. A global stocktake is instituted to assess the necessary emissions reductions every five
22 years. Here, we propose an adaptive approach to quantify successively global emissions reductions that
23 allow reaching a temperature target within $\pm 0.2^\circ\text{C}$ – solely based on regularly updated observations of
24 past temperatures, radiative forcing, and emissions statistics and not on climate model projections.
25 Testing this approach using an Earth System Model of Intermediate Complexity demonstrates that
26 defined targets can be reached following a smooth emissions pathway. The adaptive nature makes the
27 approach robust against inherent uncertainties in observational records, climate sensitivity,
28 effectiveness of emissions reduction implementations, and the metric to estimate CO₂ equivalent
29 emissions. This approach allows developing emission trajectories for CO₂, CH₄, N₂O, and other agents
30 that iteratively adapt to meet a chosen temperature target.

31 Human-made emissions of greenhouse gases (GHG) and other radiative forcing agents have led to global
32 warming of around 1.2°C by 2020¹ with already observable negative impacts on the world’s climate and
33 ecosystems^{2,3}. To limit the impact from further warming^{4,5}, 191 countries signed the Paris agreement to
34 “keep global warming well below 2°C and to pursue efforts to limit it to 1.5°C” by reducing GHG
35 emissions⁶. As a central part of the agreement, a regular five-year stocktake process was instituted to
36 assess collective progress in reducing emissions over the previous five-year period and to reassess the
37 necessary global emission reductions for the following five years and beyond. Each signatory country
38 provides its nationally determined contributions (NDCs) to the globally necessary GHG emissions
39 reductions.

40

41 These necessary reductions to reach a chosen temperature target are often derived using the concept of
42 a remaining emissions budget (REB)^{2,7-9}. Such a REB quantifies the total allowed emissions that can still be
43 emitted from the present-day onwards before a temperature target is reached. In the past, REBs usually
44 only included CO₂⁸⁻¹². Non-CO₂ forcing agents were generally included as prescribed, scenario-dependent,
45 climate forcing, bringing an additional uncertainty into the remaining carbon budget⁸⁻¹³. To consider
46 emissions of different radiative forcing agents and precursors in one budget, the concepts of Global
47 Warming Potential (GWP)¹⁴ and CO₂-forcing equivalent (CO₂-fe) emissions^{7,15,16} can be used. The GWP for
48 a time horizon of 100 years (GWP-100) is the metric applied by the parties of the Paris Agreement,
49 although GWP-100 equivalent emissions from different gases do not result in identical forcing trajectories
50 and climate impacts^{7,15,17-19} and other metrics can be additionally used for reporting²⁰. CO₂-fe emissions
51 are defined as the amount of CO₂ emissions that would cause the same radiative forcing trajectory as
52 emissions from a non-CO₂ agent (e.g., methane). Thus, the CO₂-fe metric is best suited to compare
53 emissions from different agents in the context of forcing and temperature stabilization pathways.
54 However, even when non-CO₂ emissions are transferred to CO₂-fe emissions and added to the total REB

55 and not treated as an additional uncertainty of the remaining carbon emissions budget, estimations of
56 the REB in 2020 that allows reaching the 1.5°C temperature target still *likely* vary by a factor of more than
57 two (130–300 Pg C)^{7,21}.

58

59 This range mainly stems from uncertainties in the global temperature response to changes in radiative
60 forcing agents and precursors^{8,22–25}, historical CO₂-fe emissions⁷, historical anthropogenic warming^{26–29},
61 change in temperatures after net zero CO₂-fe emissions are reached³⁰, and future sources and sinks of CO₂
62 and other agents^{30–36}. Furthermore, natural interannual-to-decadal variability in temperature^{37–39}, and
63 land and ocean carbon and heat sinks^{33,40} may mask effects of GHG emissions reductions^{41,42}.

64

65 The large REB uncertainties may hamper efforts to establish ambitious NDCs and could potentially lead to
66 insufficient global emission reductions, large global warming, and severe consequences for natural and
67 human systems^{2,43,44}. Therefore, emissions reductions should be estimated at each stocktake using
68 approaches that side-step these uncertainties and allows smoothly approaching a temperature target.
69 Such approaches should be transparent, verifiable, and, to the extent possible, objective to foster their
70 acceptance as well as the implementation of the implied near-term emissions reduction measures. Such
71 a science-based approach to guide near-term emission reduction policies is currently missing.

72

73 **The Adaptive Emissions Reduction Approach (AERA)**

74

75 Here, we propose an Adaptive Emissions Reduction Approach (AERA) to estimate the necessary emission
76 reductions until temperature stabilization successively every five years (e.g., 2025, 2030, ...) as foreseen
77 by the stocktake mechanism. By adapting emissions every five years, the AERA works like a control system
78 that corrects emissions based on the realized warming to eventually approach a prescribed temperature

79 target within a narrow range ($\pm 0.2^{\circ}\text{C}$). For example, a temperature target of 1.75°C may be chosen to
80 estimate the emissions for keeping “global warming well below 2°C ”. At a future stocktake, the
81 temperature target can be re-defined, for example “to pursue efforts to limit it to 1.5°C ”.

82

83 The AERA only relies on global surface temperature observations, radiative forcing (RF), and emissions
84 data, and does not rely on any Earth system model projections. Its adaptive nature ensures that emission
85 reductions are quantified that allow meeting the foreseen temperature target, irrespective of
86 uncertainties in understanding the climate system. Such adaptive learning and stepwise adjustment of
87 the emission reduction target has been shown to help reducing costs⁴⁵ and to avoid strong negative
88 outcomes for the economy and the environment⁴⁴.

89

90 The AERA consists of three main steps: (1) determining the past anthropogenic warming and hence the
91 remaining warming allowed, (2) estimating the remaining CO₂-fe emission budget, and (3) proposing a
92 future CO₂-fe emission curve until temperature stabilization (Figure 1; see Methods). First, the
93 anthropogenic warming is calculated from observed global mean surface temperature (GMST) time-series
94 using the past RF of all relevant forcing agents (labelled as ‘Step 1’ in Figure 1)⁴⁶. This approach removes
95 temperature changes from natural variability and non-anthropogenic forcing, such as volcanic eruptions
96 and changes in solar activity, by fitting an Impulse-Response Function^{47,48} to the RF and GMST time-series,
97 only leaving the anthropogenic contribution to the observed warming. Alternatively, natural, interannual-
98 to-decadal variability in GMST may also be removed by applying a smoothing spline or another low pass
99 filter^{49,50}. Once the realized anthropogenic warming is determined, the remaining warming between the
100 temperature target and the realized anthropogenic warming is estimated by difference.

101

102

The Adaptive Emissions Reduction Approach (AERA)

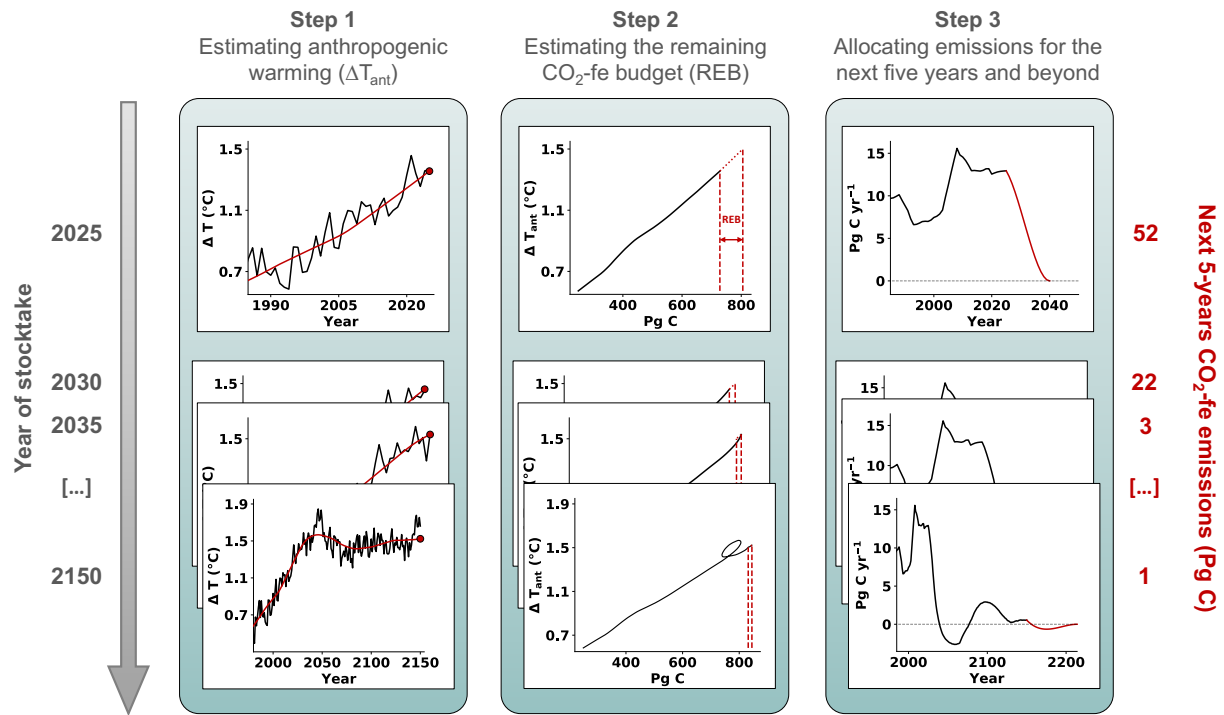


Fig. 1. Schematic of the Adaptive Emission Reduction Approach to limit global warming. The three steps are repeated at the year of each stocktake (indicated on the left) to determine allowable emissions for the next five-year period (red numbers on the right) from temperature observations and forcing and emissions statistics. The approach is illustrated using results from one Bern3D-LPX simulation with ECS=3.2°C as a surrogate for future observations (black lines in insets). Step 1: Estimation of the anthropogenic warming (red lines in inset) at the time of the stocktake from past time-series of GMST (black line) and anthropogenic radiative forcing. Step 2: Estimation of the remaining CO₂-fe emissions budget (REB; space between dashed red lines) based on the observed linear relationship between anthropogenic warming (ΔT_{ant}) and cumulative CO₂-fe emissions (black line). Step 3: Allocation of the REB over the next five years and beyond using a cubic function with minimal slope changes (red line). The approach stabilizes ΔT_{ant} close to the given target, here 1.5°C, as illustrated in the bottom left inset.

117 Second, the REB of CO₂-fe emissions is estimated using the transient climate response to cumulative
118 emissions (TCRE)^{51,52}, determined as the ratio of past warming and past cumulative CO₂-fe emissions (Step
119 2 in Figure 1). Mathematically, the REB is estimated as the remaining warming until the temperature
120 target divided by TCRE. Therefore, we rely here on the near-linear relationship between cumulative CO₂-
121 fe emission and warming over the past and the assumption that this relationship holds for the near-
122 future^{14,53}.

123
124 When quantified, the REB of CO₂-fe emissions is distributed over the future years (Step 3 in Figure 1).
125 Many possible future CO₂-fe emission curves may exist for one specific REB with different lengths and
126 economic and political assumptions⁵⁴. For simplicity, we use a cubic polynomial function and chose the
127 parameters of the cubic function and its length, i.e., the time until the REB is exhausted, by minimizing
128 the curvature. Thereby, we assume that smaller changes in the trend of CO₂-fe emission curves are easier
129 to implement. It may happen that the curve with the smallest curvature has positive emissions that are
130 later compensated by negative emissions, which would result in a temporary temperature overshoot that
131 could be harmful to the economy^{55,56} and ecosystems^{57,58}. To reduce the risk of such an overshoot, we also
132 minimized exceedance emissions, i.e., negative emissions if the REB is still positive or positive emissions
133 if the REB is negative. A negative REB can occur if the anthropogenic warming or the TCRE turns out to be
134 larger than estimated in the previous stocktakes.

135
136 The three steps of the AERA are intended to be repeated every five years at each stocktake (Figure 1). At
137 each stocktake, the determined future CO₂-fe emission curve until temperature stabilization can be split
138 into contributions from CO₂, CH₄, and N₂O emissions, as well as contributions from other non-CO₂ forcing
139 agents. This split may be achieved using a metric of choice, for example CO₂-fe emissions, which captures
140 the temperature change per CO₂-fe emissions precisely^{7,15-17} or GWP-100^{18,19,59}, which is simpler and can

141 nevertheless lead to relatively good results in terms of mitigation costs and climate outcomes^{60,61}.
142 Independent of the metric to split the CO₂-fe emissions into CO₂ and non-CO₂ emissions, the AERA adjusts
143 the future CO₂-fe emission curve every five years based on the most up-to-date observations of GMST,
144 RF, and CO₂-fe emissions. If the anthropogenic warming will turn out to be larger or smaller than
145 anticipated by the time of the next stocktake, the adaptive nature of the AERA will adjust this successively,
146 much like a control system with a feedback loop. These regular adaptations successively correct for
147 inherent uncertainties of the respective system, here the estimation of the realized anthropogenic
148 warming and the response of GMST to anthropogenic emissions.

149

150 **Testing the AERA with an Earth System Model**

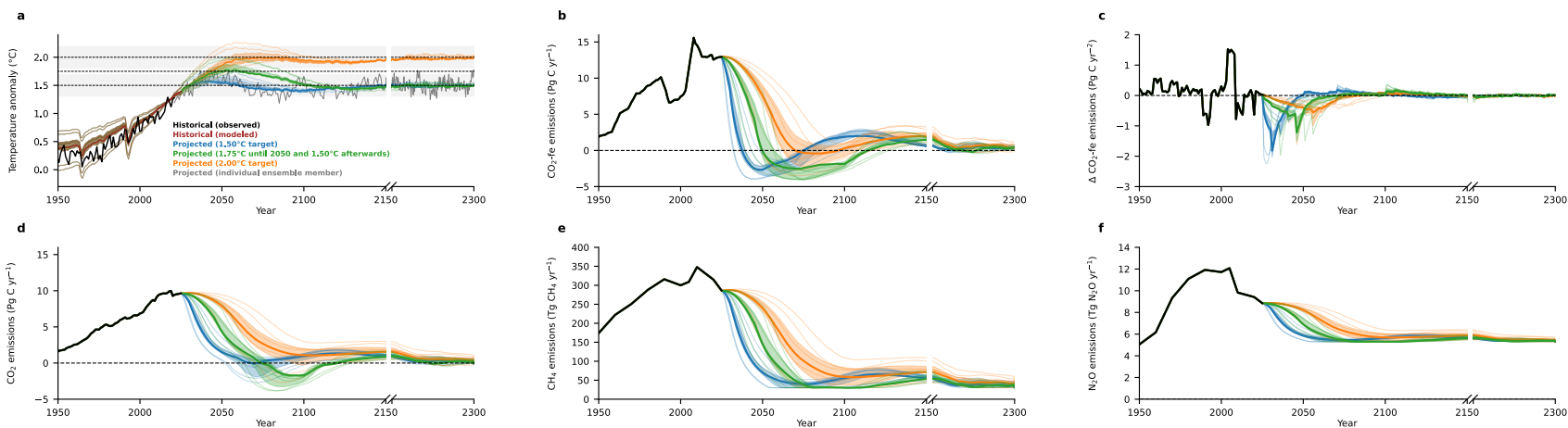
151

152 Uncertainties are not explicitly considered in a control system, c.f., the AERA, but they determine how
153 well the control system is functioning. We demonstrate that the AERA allows to reach a chosen
154 temperature level, also those well below 2°C, within the uncertainty with which the anthropogenic
155 warming can be determined ($\pm 0.2^\circ\text{C}$)²⁶⁻²⁹, independent of uncertainties in the Earth's temperature
156 sensitivity to GHGs and other agents, the strength of the land and ocean carbon sinks, radiative forcing
157 estimates, the split-up of CO₂-fe emissions in CO₂, CH₄, and N₂O emissions and the applied method (CO₂-
158 fe or GWP-100), and under deviations between emission reductions quantified by the AERA versus those
159 implemented. To that end, we used the Earth System Model of Intermediate Complexity Bern3D-LPX^{62,63}
160 under nine different configurations with varying atmospheric sensitivity to atmospheric forcing agents
161 and varying ocean mixing (see methods). These configurations cover the range of estimates of the
162 transient climate response ($1.3\text{-}2.5^\circ\text{C}$)²⁴ and equilibrium climate sensitivities ($1.9\text{-}5.7^\circ\text{C}$)²⁴ (see Methods).
163 Depending on the configuration, the simulated anthropogenic warming in 2020 with prescribed historical
164 CO₂ emissions and non-CO₂ radiative forcing ranges from 0.64 to 1.48°C versus $1.23\pm 0.20^\circ\text{C}$ from

165 observations (Extended Data Figure 1). The remaining warming in the ensemble would deviate from the
166 observational estimate when prescribing a fixed target in the model. To address the uncertainty in
167 remaining emissions, the remaining warming in 2020 is set to the observational estimate (0.27°C for the
168 1.5°C target, see Methods) regardless of their simulated warming up to 2020.

169
170 Here, we tested the AERA for two fixed temperature targets (1.5°C and 2.0°C) and for a peak and decline
171 case with a temperature target of 1.75°C until 2050 to “keep global warming well below 2°C”, but from
172 2050 onwards, the target is reduced at each stocktake by 0.025°C and reaches 1.5°C in 2100 “to pursue
173 efforts to limit it to 1.5°C”⁶. The target could be further reduced to avoid any exceedance of the 1.5°C
174 limit. The choice to which extent emissions are reduced by reducing CO₂ emissions versus reducing
175 emissions of any other agents are not dictated by the AERA. We exemplify trade-offs in emissions by
176 exploring different choices, e.g., regarding GHG and aerosol emissions reductions. In the standard
177 simulation, CO₂, CH₄, and N₂O emission curves evolve proportional in time after 2025 (Figure 2d-f). An
178 updated reduced form chemistry model⁶⁴ is used to calculate non-CO₂ GHG and aerosol radiative forcing
179 from emissions (see Methods). Eventually, the emission curves for individual agents are chosen for which
180 the resulting CO₂-fe emissions from all forcing agents match best the CO₂-fe emissions from the AERA.
181 Atmospheric CO₂ and GMST for the next five-year period are then simulated by the Bern3D-LPX model
182 using the AERA-estimated CO₂ fossil fuel emissions, non-CO₂ forcing, and CO₂ emissions from land use
183 change.

184
185 The simulations demonstrate that the AERA allows reaching a chosen temperature level almost exactly at
186 the end of the 22nd century and already within the uncertainty to which anthropogenic warming can be
187 determined ($\pm 0.2^\circ\text{C}$)^{26–29} in the second half of the 21st century independent of the model’s configuration
188 (Figure 2a). A temporal, small overshoot may occur if the REB was initially overestimated.



189

190 **Fig. 2. Globally averaged surface atmospheric temperature anomaly with respect to 1850-1900, CO₂-fe emissions, their annual rate of change, as well as CO₂,**
 191 **CH₄, and N₂O emissions following the adaptive emission reduction approach. (a)** Temperature anomalies with respect to 1850-1900, **(b)** CO₂-fe emissions, and
 192 **(c)** their annual rate of change if the AERA is applied every five years starting in the year 2025 for the 1.5°C target (blue) and the 2.0°C target (orange), as well as
 193 the AERA-calculated emission curves for the proportionally evolving **(d)** CO₂, **(e)** CH₄, and **(f)** N₂O are shown. CH₄, and N₂O emissions cannot descend below the
 194 thresholds 30 Tg CH₄ yr⁻¹ and 5.3 Tg N₂O yr⁻¹, respectively, due to the difficulty in abating CH₄ and N₂O emissions from agricultural and livestock sectors (see
 195 Methods for the choice of these thresholds). Temperature and emission curves are also shown if the AERA is applied with a temperature target of 1.75°C until
 196 2050 and from 2050 onwards this target is stepwise reduced at each stocktake to 1.5°C in 2100 (green). The thick solid lines show the average of the 8 simulations
 197 with varying magnitude and timing of added inter-annual temperature variability of the Bern3D-LPX model configuration with an ECS of 3.2°C, the thin solid lines
 198 show the same for the remaining 8 configurations covering ECS from 1.9 to 5.7°C, and the shaded area shows the range of all configurations that fall within the
 199 likely range of ECS as defined by Sherwood et al. (2020)²⁴. The grey shading in **(a)** indicates the uncertainty with which the anthropogenic warming can be
 200 determined ($\pm 0.2^\circ\text{C}$)²⁶⁻²⁹ for the 1.5°C and 2.0°C targets.

201 For the fixed 1.5°C target case, the resulting CO₂-fe emissions curves descend quickly (blue lines in Figure
202 2b), reach zero CO₂-fe emissions by 2038 (2033-2048, the central estimate is the mean over 8 simulations
203 with different superimposed interannual variability (see methods) from the ECS=3.2 model configuration,
204 and the range is the spread of the ensemble means across the remaining 8 model configurations with ECS
205 varying from 1.9°C to 5.7°C), become negative afterward, peak at -2.7 (-4.0 to -1.6) Pg C yr⁻¹, and eventually
206 converge to zero emissions after 2150. If CH₄ and N₂O emissions decrease strongly (Figures 2e,f), net
207 negative CO₂ emissions are not necessary to limit warming to 1.5°C, but CO₂ emissions still approach zero
208 emissions (Figure 2d).

209
210 For the fixed 2.0°C target, the resulting CO₂-fe emissions curves (orange lines in Figure 2b) descend less
211 rapidly, reach zero emissions by 2070 (2050-after 2300), and peak at negative emissions of -0.4 (-3.5 to
212 +1.0) Pg C yr⁻¹. The cumulative CO₂ equivalent emissions for the 2°C target, using GWP-100, are 310 Pg C
213 until 2050 and 543 Pg C until 2100, estimated from the AERA-derived CO₂, CH₄, and N₂O emissions. These
214 CO₂ equivalent emissions are similar to estimates by the Climate Action Tracker⁶⁵ when assuming that all
215 national pledges and targets are implemented (313 Pg C in 2050 and 513 Pg C in 2100), confirming that
216 stabilizing warming at 2.0°C is possible in this optimistic scenario⁶⁶. Maximum annual CO₂-fe emission
217 reductions for the 2.0°C target are considerably smaller than the necessary reductions for the 1.5°C target
218 (Figure 2c). Furthermore, the timing when zero CO₂-fe emissions need to be reached are in line with
219 previous estimates based on the time of the peak of radiative forcing⁶⁷.

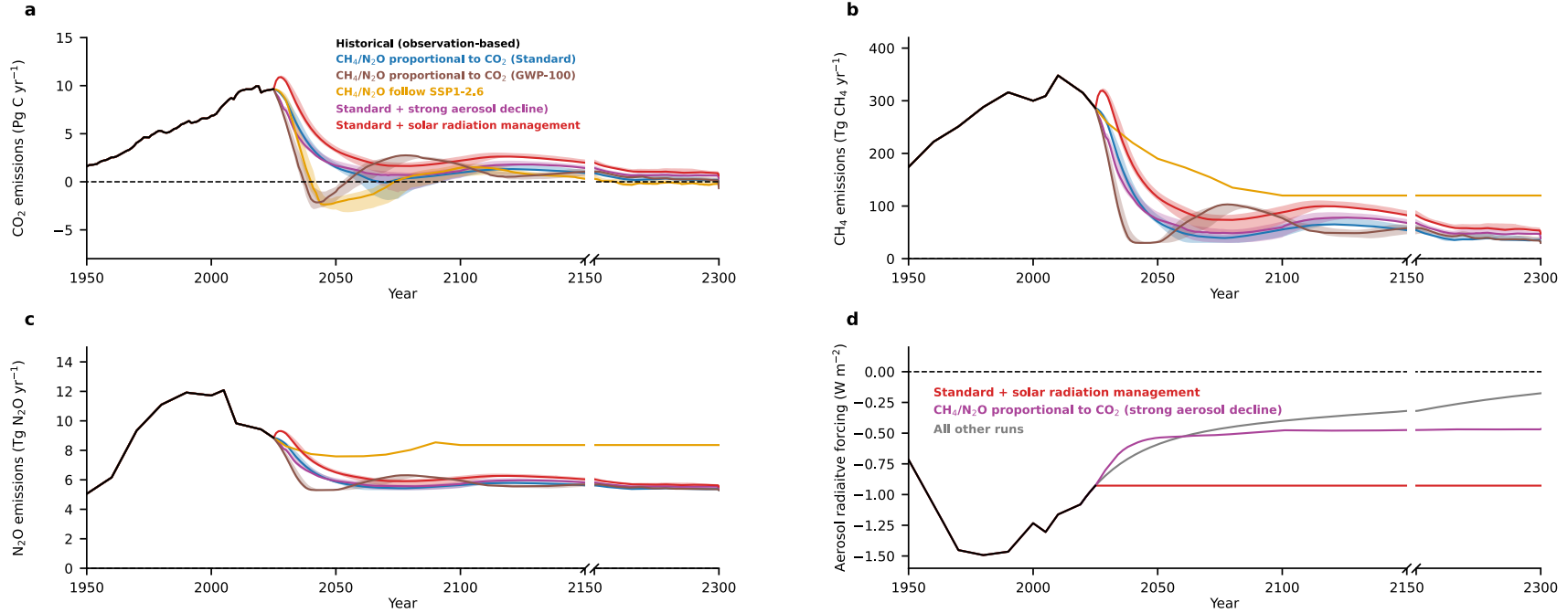
220
221 The peak and decline case demonstrates that the AERA can also be applied with a temperature target that
222 changes over time (green lines in Figure 2). In the case where the temperature target is reduced from
223 1.75°C in 2050 to 1.50°C in 2100, the 2°C warming is never exceeded. Negative CO₂-fe emissions are
224 needed until the beginning of the 22nd century. These negative CO₂-fe emissions are realized by negative

225 CO₂ emissions because CH₄ and N₂O emissions have already reached their assumed minima due to the
226 difficulty in abating CH₄ and N₂O emissions from agricultural and livestock sectors (see Methods). This
227 peak and decline simulation shows that net-zero emissions in the second half of the 21st century (Article
228 4.1 of the Paris Agreement⁶) would be sufficient to “keep global warming well below 2°C, if strong
229 emission reductions were implemented in the first half of the 21st century.

230
231 The relative smoothness of the emission curves (Figure 2b, d-f) demonstrates that the projected CO₂-fe
232 emission curves as well as the associated CO₂, CH₄ and N₂O emissions curves by the AERA will need only
233 relatively small adjustments every five years. Therefore, the longer-term projections of CO₂-fe emission
234 curves were reliable and less frequent adjustments may be sufficient. Even if CO₂-fe emission curves were
235 adjusted by the AERA only every 10 years, the resulting CO₂-fe emission curves look almost identical
236 (Extended Data Figure 2). However, small changes at every stocktake are still unavoidable as the REB
237 remains uncertain. The initial REB guess can be different from the final emissions budget because the
238 linearity between warming and cumulative emissions does not hold strictly in all configurations when
239 emissions approach zero, partly due to unrealized warming (or cooling) from past CO₂-fe emission (i.e.,
240 the zero-emission commitment³⁰) that varies between model configurations. For Bern3D-LPX,
241 temperatures decrease slightly in the decades after zero emissions are reached³⁰. This decrease is
242 automatically corrected by the AERA by slightly increasing CO₂-fe emissions. Despite these uncertainties
243 in the initial estimate of the REB, the adaptive nature of the AERA allows reaching the temperature target
244 while keeping changes in the CO₂-fe emission curve as small as possible.

245
246 Furthermore, we tested the robustness of the AERA under varying pathways of CH₄ and N₂O emission
247 curves and aerosol radiative forcing, by performing three more simulations for the 1.5°C target (Figure 3
248 - violet, red, and ochre curves). Independent of the prescribed non-CO₂ emissions and radiative agents,

249 the respective CO₂-fe emission curves remain almost indistinguishable and temperature stabilization is
250 reached by the AERA in each case (Extended Data Figure 3). However, the necessary CO₂ emission
251 reductions (Figure 3a) depend strongly on the corresponding reduction in CH₄ and N₂O emissions and
252 aerosol radiative forcing. When the magnitude of the aerosol forcing decreases faster (violet curves),
253 slightly stronger reductions in CO₂, CH₄, and N₂O emissions are needed. In an idealized 'solar radiation
254 management' case where aerosols are artificially emitted in the atmosphere after 2025 (red curves), CO₂,
255 CH₄, and N₂O emissions reductions would only need to start 10-15 years later than in the standard case
256 (blue curves), while the necessary reduction rates of CO₂, CH₄, and N₂O emissions would remain similar.
257 Moreover, once the solar radiation management would stop (not simulated here), strong reductions in
258 CO₂, CH₄, and N₂O emissions would be necessary immediately^{68,69}. In the extreme case, where only
259 emissions from non-CO₂ gases may be reduced but CO₂ remains constant, temperature cannot be
260 stabilized (Extended Data Figure 4). Although reductions of non-CO₂ emissions can compensate for
261 reductions in CO₂ emissions for some decades, continuing CO₂ emissions will lead to further increases
262 atmospheric CO₂ and hence the global temperature.



263

264 **Fig. 3. Emissions of CO₂, CH₄, and N₂O, and aerosol radiative forcing following the adaptive emission reduction approach for the 1.5°C temperature target**
 265 **using different assumptions for non-CO₂ radiative forcing agents. (a) CO₂ emissions, (b) CH₄ emissions, (c) N₂O emissions, and (d) the total radiative forcing of**
 266 **anthropogenic aerosols (stratospheric and tropospheric) for five different idealized cases: aerosol radiative forcing decreases exponentially and CO₂, CH₄, and**
 267 **N₂O emissions evolve proportionally (blue), aerosol radiative forcing decreases exponentially and CO₂, CH₄, and N₂O emissions evolve proportionally but GWP-**
 268 **100 is used to split CO₂ equivalent emissions instead of the CO₂-fe approach (brown), aerosol radiative forcing decreases stronger due to strong CO₂ emissions**
 269 **cuts^{71,72} and CO₂, CH₄, and N₂O emissions evolve proportionally (violet), aerosol radiative forcing decreases exponentially but CH₄, and N₂O emissions follow SSP1-**
 270 **2.6 after 2025 and only CO₂ evolves dynamically (ochre), and aerosol radiative forcing remains constant after 2025 and CO₂, CH₄, and N₂O emissions evolve**
 271 **proportionally (red, idealized solar radiation management). The thick solid lines show the average of the 8 simulations with varying magnitude and timing of**

272 added inter-annual temperature variability of the Bern3D-LPX model configuration with an ECS of 3.2°C and the shaded area shows the range of all configurations
273 that fall within the likely range of ECS as defined by Sherwood et al. (2020)²⁴. The corresponding temperature curves, CO₂-fe emissions, and CO₂-e emissions for
274 each simulated case are shown in Extended Data Figure 3.

275 The almost identical temperature curves and associated CO₂-fe emission curves across these four
276 scenarios with varying CH₄, and N₂O emissions as well as varying radiative forcing from aerosols (Extended
277 Data Figure 3) highlights the robustness of the CO₂-fe approach for transferring contributions from
278 different radiative forcing agents to CO₂ equivalent emissions^{7,15-17}. However, as the GWP-100 approach
279 is widely used, e.g., in the Paris Agreement, we tested the AERA using GWP-100 by repeating the standard
280 simulations but using the GWP-100 and not the CO₂-fe metric to transfer CH₄ and N₂O emissions to CO₂
281 equivalent emissions (brown curves in Figure 3). The AERA stabilizes the temperature at the given target
282 when using GWP-100 (Extended Data Figure 5). However, the limitations^{7,15,17-19} of the GWP-100 metric
283 lead to an overcorrection at first of the CO₂, CH₄, and N₂O emissions reductions by the AERA by up to 78%
284 for CO₂ (maximum relative difference in emissions reductions since 2025) and 46% for CH₄ and N₂O that
285 is later corrected by positive CO₂-fe emissions (brown curves in Figure 3 and Extended Data Figure 5b-f).
286 However, when the usage of GWP is envisioned, better results may be achieved by using temperature
287 change potentials⁷⁰ or adjustments to the GWP over time⁶¹.

288
289 The behavior of the AERA was further investigated assuming precautionary “over-compliance” (using a
290 REB that is smaller than the central estimate, i.e., 67th and 83rd percentile instead of the 50th percentile)
291 or “under-compliance” (using a REB that is higher than the central estimate, i.e., 17th and 33rd percentile).
292 In the case of “under-compliance”, the target temperature is still reached, but at the cost of a larger
293 temperature overshoot (Extended Data Figures 6 and 7). In the case of “over-compliance”, the
294 temperature target is also reached, and the temperature overshoot can be avoided or reduced (for the
295 highest ECS). Overall, the AERA thus provides a robust and working tool to estimate the necessary
296 emission reductions to minimize the risk of temperature overshoot and the risk to surpass a given
297 temperature limit, e.g., of 2°C.

298

299 **Applying the AERA in 2020**

300

301 Having demonstrated the robustness and fidelity of the AERA in the model world, the question arises what
302 rate of emission reductions the AERA would have estimated for the 1.5°C and 2.0°C temperature targets
303 based on available observations and emissions statistics in 2020, when 186 parties had communicated
304 their first NDCs to the United Nations Framework Convention on Climate Change (UNFCCC) Secretariat.
305 Applied to observational data until 2020, step one of the AERA yields an anthropogenic warming of 1.23°C
306 resulting in a remaining warming of 0.27°C for the 1.5°C target and 0.77°C for the 2.0°C target. In step 2,
307 the ratio of the anthropogenic warming of 1.23°C and past cumulative CO₂-fe emissions of 749 Pg C results
308 in an REB of 167 Pg C for 1.5°C and 472 Pg C for 2.0°C. These remaining CO₂-fe emissions are divided over
309 the coming years in step 3 of the AERA assuming a cubic polynomial function with minimum changes of
310 its slope. The so estimated reduction of annual CO₂-fe emissions from 2020 to 2025 is 3.7 Pg C for the
311 1.5°C temperature target (from 13.7 Pg C yr⁻¹ in 2020 to 10.0 Pg C yr⁻¹ in 2025) and 1.0 Pg C for the 2.0°C
312 temperature target (from 13.7 Pg C yr⁻¹ in 2020 to 12.6 Pg C yr⁻¹ in 2025). Beyond 2025, CO₂-fe emissions
313 would have to drop to 7.0 Pg C yr⁻¹ in 2030 to reach the 1.5°C target, further decrease to 0.5 Pg C yr⁻¹ in
314 2050 and become lightly negative after 2055 (up to -0.5 Pg C yr⁻¹) until reaching zero CO₂-fe emissions in
315 2085. For the 2.0°C target, CO₂-fe emissions would have to reach 11.3 Pg C yr⁻¹ in 2030, 7.2 Pg C yr⁻¹ in
316 2050 and zero CO₂-fe emissions by 2110. While the estimates of past warming, TCRE, REB, and necessary
317 emission reductions have uncertainties, the AERA side-steps these uncertainties. The successive
318 adaptation of the CO₂-fe emissions every five years allows to correct the emission pathway over time if
319 the initial estimates were not exact. Estimates are based on the median (50th percentile) value in these
320 example calculations for year 2020. Other percentiles may be used, as in the “overcompliance case”
321 described previously, for considering the precautionary principle of the UNFCCC.^{71,72}

322

323 **Discussion**

324

325 The AERA allows estimating future CO₂-fe emission pathways to reach the desired temperature target
326 within the uncertainty to which anthropogenic warming can be determined ($\pm 0.2^\circ\text{C}$)²⁶⁻²⁹. Climate
327 projections by Earth System Models using the AERA could be incorporated into the periodical IPCC
328 Assessment Reports and provide an alternative to the often-used approach of applying pre-defined
329 emissions or concentration pathways (such as SSPs). Such pathways are generally designed a priori to be
330 consistent with a given radiative forcing or warming level (e.g., SSP1-1.9 for 1.9 W m^{-2} and 1.5°C by 2100),
331 not knowing the actual response of the Earth system to these emissions pathways⁷³. AERA-based warming
332 simulations from different models would be directly comparable in terms of impacts under equal
333 warming. However, the sociotechnical feasibility of the pathways is not informed by the AERA but could
334 be assessed by coupling these simulations to a cost-effectiveness integrative assessment model in a
335 recursive dynamic setup. The approach may hence guide a valuable and highly policy-relevant
336 complementary set of simulations for the next generation of CMIP models that result in a range of
337 emission curves that all result in the same warming in the long term as opposed to current simulations
338 with the same emission or concentration curves that can result in very different levels of warming.

339

340 In the Paris Agreement, the 2°C warming limit represents an upper threshold that should not be passed.
341 The AERA applied with the median observation-based estimates allows to devise pathways that keep
342 warming to within about 0.2°C of prescribed warming targets. For keeping warming below temperature
343 limits that have been set as upper ceilings for global warming allowable to society, the AERA can be
344 applied with a temperature target about 0.2°C lower than such limits or by using a lower than the median
345 estimate for the REB as in the “overcompliance case”. In future efforts, the approach could be further

346 refined by applying the AERA within a fully observation-constrained probabilistic framework^{12,13} to
347 estimate the necessary emission reductions with associated likelihoods.

348

349 The AERA presents policy makers transparent science- and observation-based emission reductions that
350 would be necessary to limit global warming to any chosen temperature level without the need to make
351 climate projections with Earth System Models. With many simulations, substituting for future real-world
352 outcomes, we have shown that this approach is robust across a vast number of possible developments.
353 Policy makers may wish to use the information from the AERA to regularly update near- and long-term
354 emission reduction goals, including additional socio-economic considerations such as equity, mitigation
355 versus adaptation costs, and risks of not meeting a target. The AERA can thereby help to successfully “keep
356 global warming well below 2°C and to pursue efforts to limit it to 1.5°C”⁶.

357

358 **Data availability**

359 The Bern3D-LPX model output is available publicly available via SEANOE
360 (<https://doi.org/10.17882/90901>)⁷⁴. All other data are available in the main text or the supplementary
361 materials.

362

363 **Code availability**

364 The AERA code is publicly available via <https://github.com/Jete90/AERA>⁷⁵.

365

366 **Acknowledgements**

367 We thank Piers Forster, Joeri Rogelj, and an unknown reviewer for their valuable comments. This work
368 was funded by the European Union's Horizon 2020 research and innovation programme under grant
369 agreement No 821003 (project 4C, Climate-Carbon Interactions in the Current Century) (JT, TLF, FJ, PF),
370 and grant agreement No 101003687 (project PROVIDE, Paris Agreement Overshooting) (TLF), and by the
371 Swiss National Science Foundation under grant PP00P2_198897 (TLF) and grant #200020_200511 (FJ). The
372 work reflects only the authors' view; the European Commission and their executive agency are not
373 responsible for any use that may be made of the information the work contains. We thank Damien Guignet
374 for initial analysis, Sebastian Lienert and Aurich Jeltsch-Thömmes for help with Bern3D-LPX, and the 4C
375 partners for helpful discussions.

376

377 **Author Contributions**

378 Conceptualization: JT, TLF, FJ, PF

379 Methodology: JT, MA, TLF, FJ

380 Software: JT, MA

381 Investigation: JT

382 Visualization: JT, TLF, FJ

383 Funding acquisition: TLF, FJ, PF

384 Project administration: TLF, FJ

385 Writing – original draft: JT

386 Writing – review & editing: JT, MA, TLF, FJ, PF

387

388 **Author information/Competing Interests**

389 Authors declare that they have no competing interests.

390 **References**

- 391 1. World Meteorological Organization. *State of the Global Climate 2020*.
392 https://library.wmo.int/doc_num.php?explnum_id=10618 (2021).
- 393 2. Allen, M. R. *et al.* Framing and Context. in *Global warming of 1.5°C* (eds. Masson-
394 Delmotte, V. et al.) (2018).
- 395 3. IPCC. *Special Report on the Ocean and Cryosphere in a Changing Climate*. (2019).
- 396 4. Hoegh-Guldberg, O. *et al.* The human imperative of stabilizing global climate change at
397 1.5°C. *Science (1979)* **365**, eaaw6974 (2019).
- 398 5. Hoegh-Guldberg, O. *et al.* Impacts of 1.5°C of Global Warming on Natural and Human
399 Systems. in *Global warming of 1.5°C* (eds. Masson-Delmotte, V. et al.) (2018).
- 400 6. UNFCCC. *Paris agreement. Report of the Conference of the Parties to the United Nations*
401 *Framework Convention on Climate Change*. (2015).
- 402 7. Jenkins, S., Millar, R. J., Leach, N. & Allen, M. R. Framing Climate Goals in Terms of
403 Cumulative CO₂-Forcing-Equivalent Emissions. *Geophys Res Lett* **45**, 2795–2804 (2018).
- 404 8. Rogelj, J., Forster, P. M., Kriegler, E., Smith, C. J. & Séférian, R. Estimating and tracking the
405 remaining carbon budget for stringent climate targets. *Nature* **571**, 335–342 (2019).
- 406 9. Matthews, H. D. *et al.* Opportunities and challenges in using remaining carbon budgets to
407 guide climate policy. *Nat Geosci* **13**, 769–779 (2020).
- 408 10. Tokarska, K. B. & Gillett, N. P. Cumulative carbon emissions budgets consistent with 1.5 °C
409 global warming. *Nat Clim Chang* **8**, 296–299 (2018).
- 410 11. Peters, G. P. Beyond carbon budgets. *Nat Geosci* **11**, 378–380 (2018).
- 411 12. Damon Matthews, H. *et al.* An integrated approach to quantifying uncertainties in the
412 remaining carbon budget. *Commun Earth Environ* **2**, 7 (2021).
- 413 13. Steinacher, M., Joos, F. & Stocker, T. F. Allowable carbon emissions lowered by multiple
414 climate targets. *Nature* **499**, 197–201 (2013).
- 415 14. IPCC. Summary for Policymakers. in
416 *Climate Change 2013: The Physical Science Basis. Contribution of Working Group I to*
417 *the Fifth Assessment Report of the Intergovernmental Panel on Climate Change* (eds.
418 Stocker, T. F. et al.) (Cambridge University Press, 2013).
- 419 15. Allen, M. R. *et al.* A solution to the misrepresentations of CO₂-equivalent emissions of
420 short-lived climate pollutants under ambitious mitigation. *NPJ Clim Atmos Sci* **1**, 16 (2018).

- 421 16. Wigley, T. M. L. The Kyoto Protocol: CO₂ CH₄ and climate implications. *Geophys Res Lett*
422 **25**, 2285–2288 (1998).
- 423 17. Smith, M. A., Cain, M. & Allen, M. R. Further improvement of warming-equivalent
424 emissions calculation. *NPJ Clim Atmos Sci* **4**, 19 (2021).
- 425 18. Tanaka, K. & O’Neill, B. C. The Paris Agreement zero-emissions goal is not always
426 consistent with the 1.5 °C and 2 °C temperature targets. *Nat Clim Chang* **8**, 319–324
427 (2018).
- 428 19. Allen, M. *et al.* Ensuring that offsets and other internationally transferred mitigation
429 outcomes contribute effectively to limiting global warming. *Environmental Research*
430 *Letters* **16**, 74009 (2021).
- 431 20. *Paragraphs 37 of the Addendum to UNFCCC Decision 18/CMA.1, agreed at the COP24 in*
432 *December 2018.*
- 433 21. Arias, P. A. *et al.* Technical Summary. in *Climate Change 2021: The Physical Science Basis.*
434 *Contribution of Working Group I to the Sixth Assessment Report of the Intergovernmental*
435 *Panel on Climate Change* (eds. Masson-Delmotte, V. *et al.*) (Cambridge University Press,
436 2021).
- 437 22. A, M. G. *et al.* Context for interpreting equilibrium climate sensitivity and transient climate
438 response from the CMIP6 Earth system models. *Sci Adv* **6**, eaba1981 (2022).
- 439 23. Nijse, F. J. M. M., Cox, P. M. & Williamson, M. S. Emergent constraints on transient
440 climate response (TCR) and equilibrium climate sensitivity (ECS) from historical warming in
441 CMIP5 and CMIP6 models. *Earth System Dynamics* **11**, 737–750 (2020).
- 442 24. Sherwood, S. C. *et al.* An Assessment of Earth’s Climate Sensitivity Using Multiple Lines of
443 Evidence. *Reviews of Geophysics* **58**, e2019RG000678 (2020).
- 444 25. Tokarska Katarzyna, B. *et al.* Past warming trend constrains future warming in CMIP6
445 models. *Sci Adv* **6**, eaaz9549 (2021).
- 446 26. Haustein, K. *et al.* A real-time Global Warming Index. *Sci Rep* **7**, 15417 (2017).
- 447 27. Ribes, A., Qasmi, S. & Gillett, N. P. Making climate projections conditional on historical
448 observations. *Sci Adv* **7**, eabc0671 (2022).
- 449 28. Gillett, N. P. *et al.* Constraining human contributions to observed warming since the pre-
450 industrial period. *Nat Clim Chang* **11**, 207–212 (2021).
- 451 29. IPCC. Summary for Policymakers. in *Climate Change 2021: The Physical Science Basis.*
452 *Contribution of Working Group I to the Sixth Assessment Report of the Intergovernmental*

- 453 *Panel on Climate Change* (eds. Masson-Delmotte, V. et al.) (Cambridge University Press,
454 2021).
- 455 30. MacDougall, A. H. *et al.* Is there warming in the pipeline? A multi-model analysis of the
456 Zero Emissions Commitment from CO₂. *Biogeosciences* **17**, 2987–3016 (2020).
- 457 31. Saunio, M. *et al.* The Global Methane Budget 2000–2017. *Earth Syst Sci Data* **12**, 1561–
458 1623 (2020).
- 459 32. Heinze, C. *et al.* ESD Reviews: Climate feedbacks in the Earth system and prospects for
460 their evaluation. *Earth System Dynamics* **10**, 379–452 (2019).
- 461 33. Friedlingstein, P. *et al.* Global Carbon Budget 2020. *Earth Syst Sci Data* **12**, 3269–3340
462 (2020).
- 463 34. Arora, V. K. *et al.* Carbon–concentration and carbon–climate feedbacks in CMIP6 models
464 and their comparison to CMIP5 models. *Biogeosciences* **17**, 4173–4222 (2020).
- 465 35. Jones, C. D. & Friedlingstein, P. Quantifying process-level uncertainty contributions to
466 TCRE and carbon budgets for meeting Paris Agreement climate targets. *Environmental*
467 *Research Letters* **15**, 074019 (2020).
- 468 36. Tian, H. *et al.* A comprehensive quantification of global nitrous oxide sources and sinks.
469 *Nature* **586**, 248–256 (2020).
- 470 37. Thompson, D. W. J., Wallace, J. M., Jones, P. D. & Kennedy, J. J. Identifying Signatures of
471 Natural Climate Variability in Time Series of Global-Mean Surface Temperature:
472 Methodology and Insights. *J Clim* **22**, 6120–6141 (2009).
- 473 38. Medhaug, I., Stolpe, M. B., Fischer, E. M. & Knutti, R. Reconciling controversies about the
474 ‘global warming hiatus’. *Nature* **545**, 41–47 (2017).
- 475 39. Turner, J. *et al.* Absence of 21st century warming on Antarctic Peninsula consistent with
476 natural variability. *Nature* **535**, 411–415 (2016).
- 477 40. Watanabe, M. *et al.* Strengthening of ocean heat uptake efficiency associated with the
478 recent climate hiatus. *Geophys Res Lett* **40**, 3175–3179 (2013).
- 479 41. Peters, G. P. *et al.* Towards real-time verification of CO₂ emissions. *Nat Clim Chang* **7**,
480 848–850 (2017).
- 481 42. Spring, A., Ilyina, T. & Marotzke, J. Inherent uncertainty disguises attribution of reduced
482 atmospheric CO₂ growth to CO₂ emission reductions for up to a decade. *Environmental*
483 *Research Letters* **15**, 114058 (2020).

- 484 43. Steffen, W. *et al.* Trajectories of the Earth System in the Anthropocene. *Proceedings of the*
485 *National Academy of Sciences* **115**, 8252 (2018).
- 486 44. Oppenheimer, M., O'Neill, B. C. & Webster, M. Negative learning. *Clim Change* **89**, 155–
487 172 (2008).
- 488 45. Webster, M., Jakobovits, L. & Norton, J. Learning about climate change and implications
489 for near-term policy. *Clim Change* **89**, 67–85 (2008).
- 490 46. Otto, F. E. L., Frame, D. J., Otto, A. & Allen, M. R. Embracing uncertainty in climate change
491 policy. *Nat Clim Chang* **5**, 917–920 (2015).
- 492 47. Held, I. M. *et al.* Probing the Fast and Slow Components of Global Warming by Returning
493 Abruptly to Preindustrial Forcing. *J Clim* **23**, 2418–2427 (2010).
- 494 48. Joos, F. *et al.* Carbon dioxide and climate impulse response functions for the computation
495 of greenhouse gas metrics: a multi-model analysis. *Atmos Chem Phys* **13**, 2793–2825
496 (2013).
- 497 49. Enting, I. G. On the use of smoothing splines to filter CO₂ data. *Journal of Geophysical*
498 *Research: Atmospheres* **92**, 10977–10984 (1987).
- 499 50. Luo, J., Ying, K. & Bai, J. Savitzky–Golay smoothing and differentiation filter for even
500 number data. *Signal Processing* **85**, 1429–1434 (2005).
- 501 51. Allen, M. R. *et al.* Warming caused by cumulative carbon emissions towards the trillionth
502 tonne. *Nature* **458**, 1163–1166 (2009).
- 503 52. Matthews, H. D., Gillett, N. P., Stott, P. A. & Zickfeld, K. The proportionality of global
504 warming to cumulative carbon emissions. *Nature* **459**, 829–832 (2009).
- 505 53. IPCC. Summary for Policymakers. in *Climate Change 2014: Synthesis Report. Contribution*
506 *of Working Groups I, II and III to the Fifth Assessment Report of the Intergovernmental*
507 *Panel on Climate Change* (eds. Pachauri, R. K. & Meyer, L. A.) (IPCC, 2014).
- 508 54. Edwards, M. R., McNerney, J. & Trancik, J. E. Testing emissions equivalency metrics
509 against climate policy goals. *Environ Sci Policy* **66**, 191–198 (2016).
- 510 55. Ricke, K. L., Millar, R. J. & MacMartin, D. G. Constraints on global temperature target
511 overshoot. *Sci Rep* **7**, 14743 (2017).
- 512 56. Parry, M., Lowe, J. & Hanson, C. Overshoot, adapt and recover. *Nature* **458**, 1102–1103
513 (2009).
- 514 57. Anderson, C. M. *et al.* Planning for Change: Conservation-Related Impacts of Climate
515 Overshoot. *Bioscience* **70**, 115–118 (2020).

- 516 58. de Vrese, P. & Brovkin, V. Timescales of the permafrost carbon cycle and legacy effects of
517 temperature overshoot scenarios. *Nat Commun* **12**, 2688 (2021).
- 518 59. Myhre, G. *et al.* Anthropogenic and Natural Radiative Forcing. in *Climate Change 2013:*
519 *The Physical Science Basis. Contribution of Working Group I to the Fifth Assessment Report*
520 *of the Intergovernmental Panel on Climate Change* (eds. Stocker, T. F. *et al.*) (Cambridge
521 University Press, 2013).
- 522 60. Harmsen, M. J. H. M. *et al.* How climate metrics affect global mitigation strategies and
523 costs: a multi-model study. *Clim Change* **136**, 203–216 (2016).
- 524 61. Tanaka, K., Boucher, O., Ciais, P., Johansson, D. J. A. & Morfeldt, J. Cost-effective
525 implementation of the Paris Agreement using flexible greenhouse gas metrics. *Sci Adv* **7**,
526 eabf9020 (2022).
- 527 62. Roth, R., Ritz, S. P. & Joos, F. Burial-nutrient feedbacks amplify the sensitivity of
528 atmospheric carbon dioxide to changes in organic matter remineralisation. *Earth System*
529 *Dynamics* **5**, 321–343 (2014).
- 530 63. Lienert, S. & Joos, F. A Bayesian ensemble data assimilation to constrain model
531 parameters and land-use carbon emissions. *Biogeosciences* **15**, 2909–2930 (2018).
- 532 64. Joos, F. *et al.* Global warming feedbacks on terrestrial carbon uptake under the
533 Intergovernmental Panel on Climate Change (IPCC) Emission Scenarios. *Global*
534 *Biogeochem Cycles* **15**, 891–907 (2001).
- 535 65. Climate Action Tracker . [https://climateactiontracker.org/documents/853/CAT_2021-05-](https://climateactiontracker.org/documents/853/CAT_2021-05-04_Briefing_Global-Update_Climate-Summit-Momentum.pdf)
536 [04_Briefing_Global-Update_Climate-Summit-Momentum.pdf](https://climateactiontracker.org/documents/853/CAT_2021-05-04_Briefing_Global-Update_Climate-Summit-Momentum.pdf).
- 537 66. Meinshausen, M. *et al.* Realization of Paris Agreement pledges may limit warming just
538 below 2 °C. *Nature* **604**, 304–309 (2022).
- 539 67. Wigley, T. M. L. The relationship between net GHG emissions and radiative forcing with an
540 application to Article 4.1 of the Paris Agreement. *Clim Change* **169**, 13 (2021).
- 541 68. Wigley, T. M. L. A Combined Mitigation/Geoengineering Approach to Climate
542 Stabilization. *Science (1979)* **314**, 452–454 (2006).
- 543 69. Robock, A., Oman, L. & Stenchikov, G. L. Regional climate responses to geoengineering
544 with tropical and Arctic SO₂ injections. *Journal of Geophysical Research: Atmospheres*
545 **113**, (2008).
- 546 70. Shine, K. P., Berntsen, T. K., Fuglestvedt, J. S., Skeie, R. B. & Stuber, N. Comparing the
547 climate effect of emissions of short- and long-lived climate agents. *Philosophical*

- 548 *Transactions of the Royal Society A: Mathematical, Physical and Engineering Sciences* **365**,
549 1903–1914 (2007).
- 550 71. Rogelj, J. *et al.* Air-pollution emission ranges consistent with the representative
551 concentration pathways. *Nat Clim Chang* **4**, 446–450 (2014).
- 552 72. Lamboll, R. D., Nicholls, Z. R. J., Kikstra, J. S., Meinshausen, M. & Rogelj, J. Silicone v1.0.0:
553 an open-source Python package for inferring missing emissions data for climate change
554 research. *Geosci Model Dev* **13**, 5259–5275 (2020).
- 555 73. O’Neill, B. C. *et al.* The Scenario Model Intercomparison Project (ScenarioMIP) for CMIP6.
556 *Geosci Model Dev* **9**, 3461–3482 (2016).
- 557 74. Terhaar, J., Frölicher, T. L., Aschwanden, M. & Joos, F. Bern3D-LPX simulations with the
558 the adaptive emission reduction approach (AERA). SEANOE.
559 <https://doi.org/10.17882/90901>
- 560 75. Terhaar, J., Frölicher, T. L., Aschwanden, M. & Joos, F. Adaptive emission reduction
561 approach (AERA). Preprint at <https://doi.org/10.5281/zenodo.7186275> (2022).
562

563 **Methods**

564

565 Adaptive Emission Reduction Approach

566

567 The Adaptive Emission Reduction Approach (AERA)⁷⁵ is designed to estimate a future trajectory of CO₂
568 forcing equivalent (CO₂-fe) emissions to reach a temperature target. The AERA is formulated as part of a
569 control system with a feedback loop. In a control system, the output of a system is controlled by regularly
570 adjusting the input to the system based on the deviation between the actual and target value of a process
571 variable. An example is a regulation of room temperature with a heating-cooling unit. The room
572 temperature is measured to estimate the deviation between the actual and target temperature. The flow
573 of heat between the unit and the room is then adjusted by the “controller” based on the deviation and
574 the median available estimate of the response in room temperature to heat flow. This procedure is
575 repeated, e.g., every minute, to adjust the room temperature towards and to track the target
576 temperature. Similarly, the AERA, when implemented with real-world emissions, will control the evolution
577 of anthropogenic warming by adjusting CO₂-fe emissions. Here, emissions are foreseen to be adjusted
578 every five years, based on the median observational estimate of the deviation between actual and target
579 anthropogenic warming and the median observation-based estimate of the Earth system’s response to
580 emissions. Implementing the regularly updated emissions reductions following the AERA will allow the
581 temperature to converge towards the target temperature, despite uncertainties in our understanding of
582 the Earth System.

583

584 As input, the AERA requires past global time-series of three variables: (i) global mean surface temperature
585 (GMST), (ii) total anthropogenic radiative forcing (RF), and (iii) total CO₂-fe emissions from CO₂, non-CO₂
586 GHGs, precursors, aerosols, and land-use change combined (see CO₂-fe emissions calculation below). The

587 AERA contains three steps. First, internal variability from the GMST record is removed by calculating
 588 anthropogenic warming from the GMST timeseries⁴⁶. Second, the Remaining CO₂-fe Emission Budget
 589 (REB)^{2,7-9} is estimated based on the near-linear relationship between past CO₂-fe emissions and warming
 590 (i.e., the transient climate response to cumulative carbon emission)^{51,52}, and the remaining temperature
 591 gap before the target temperature will be reached. Third, this REB is distributed over the future years
 592 using a cubic polynomial function. The three steps are to be repeated every five years. Therefore, the
 593 future CO₂-fe emission curve may be adjusted every five years based on the most up-to-date observations
 594 of GMST, RF, and CO₂-fe emissions.

595
 596 In the first step, the natural internal and external (i.e., volcanoes, solar activity) variability is removed from
 597 the observed, historical GMST resulting in a temperature curve (T_{ant}) that only changes due to
 598 anthropogenic forcing. T_{ant} is determined following Otto et al.⁴⁶ by fitting an Impulse-Response Function
 599 (IRF)^{47,48} to the observed GMST(t). The IRF features three characteristic timescales, τ_i , and coefficients, a_i :

600
 601
$$T_{ant}(t) = T_{ant}(1850) + c \int_{1850}^t I_{RF}(t') \left(a_1 \left(1 - e^{-\frac{-(t-t')}{\tau_1}} \right) + a_2 \left(1 - e^{-\frac{-(t-t')}{\tau_2}} \right) + a_3 \left(1 - e^{-\frac{-(t-t')}{\tau_3}} \right) \right) dt' \quad (1)$$

602
 603 Eq. 1 relates the sum of step-like changes in RF (impulses $I_{RF}(t')$, defined as the change in RF in year t') over
 604 the past observed period to $T_{ant}(t)$. The constant c is a scaling and unit conversion factor, and the integral
 605 is approximated by the sum of annual values. The seven free parameters of Eq. 1 (*timescales* τ_1 , τ_2 , and τ_3 ;
 606 *coefficients* a_1 , a_2 ; c ; $T_{ant}(1850)$) are determined to best fit the observation-based GMST by minimizing
 607 the root-mean-square-deviations between $T_{ant}(t)$ and $GMST(t)$. The parameters are determined at each
 608 stocktake to account for possible feedbacks from the warming of the climate and cumulative CO₂ uptake
 609 that may change the shape of the IRF⁷⁶. The free parameters were constrained a priori to ease the fitting.

610 The timescales are limited to 1.5-2.0 years (for τ_1), 15-30 years (τ_2), and 100-600 years (τ_3) and the
 611 coefficients are limited to 0.2-0.4 (a_1), 0.3-0.5 (a_2). a_3 is calculated by $a_3 = 1 - a_1 - a_2$. Implicitly, a_3 is thus
 612 limited to 0.1-0.5. These broad constraints are enforced to ensure physically meaningful parameters.
 613 From the anthropogenic temperature time-series $T_{ant}(t)$, the anthropogenic temperature anomaly (ΔT_{ant})
 614 is calculated by subtracting the mean $GMST(t)$ over the reference period 1850-1900 from T_{ant} :

$$616 \Delta T_{ant}(t) = T_{ant}(t) - \overline{GMST(1850 - 1900)} \quad (2)$$

617
 618 The Remaining Emission Budget (REB) of CO₂-fe emissions is estimated at the time of the stocktake, t_{st}
 619 (years 2025, 2030, ...) exploiting the near-linearity between warming and cumulative CO₂ emissions
 620 discussed by the Intergovernmental Panel on Climate Change^{14,53}. The REB (t_{st}) is determined by
 621 multiplying the remaining anthropogenic temperature anomaly until the target temperature is reached
 622 with the ratio of cumulative CO₂-fe emissions since 1850 ($\int_{1850}^{t_{st}} E_{fe}^{CO_2}(t') dt'$) and the realized anthropogenic
 623 warming anomaly $\Delta T_{ant}(t_{st})$ ^{51,52}:

$$625 REB(t_{st}) = \left(\Delta T_{ant}^{target} - \Delta T_{ant}(t_{st}) \right) \frac{\int_{1850}^{t_{st}} E_{fe}^{CO_2}(t') dt'}{\Delta T_{ant}(t_{st})}, \quad (3)$$

626
 627 with ΔT_{ant}^{target} being the temperature target, e.g., 1.5°C or 2°C.

628
 629 The emission pathway for the five years following the stocktake is determined by distributing the
 630 remaining CO₂-fe emission budget over the future years using a cubic polynomial function:

$$632 E_{fe}^{CO_2}(t) = at^3 + bt^2 + ct + d \quad \text{for } t_{target} \geq t \geq t_{st} , \quad (4)$$

633

634 with t referring to the time after the year of the stocktake (t_{st}) and t_{target} being the year when the
 635 temperature target should be reached. The t_{target} is not an a priori fixed year^{61,70} but continuous to evolve
 636 over time and will be adapted here to ensure that the change of the slope of CO₂-fe emissions remains as
 637 small as possible (see paragraph below). The parameters a , b , c , and d are chosen to determine an
 638 emission curve with a small curvature using the following boundary conditions:

639

640 1) $E_{fe}^{CO_2}(t_{st})$ equals the CO₂-fe emissions at the year of the stocktake.

641 2) Changes in $E_{fe}^{CO_2}$ in the year before the stocktake are as close as possible to changes in $E_{fe}^{CO_2}$ at
 642 the year of the stocktake:

$$643 \quad \frac{\partial E_{fe}^{CO_2}}{\partial t}(t_{st}) = \frac{\partial E_{fe}^{CO_2}}{\partial t}(t_{st} - 1) + \eta, \quad (5)$$

644 with η being a change in the slope.

645 3) $E_{fe}^{CO_2}(t_{target})$ equals zero.

646 4) $E_{fe}^{CO_2}$ remains constant after the target year is reached ($\frac{\partial E_{fe}^{CO_2}}{\partial t}(t_{target}) = 0$)

647

648 Condition 1) enforces the polynomial function to match emissions at the time of the stocktake. Condition
 649 2) minimizes the changes in the emissions trend around the stocktake, thereby implicitly accounting for
 650 inertia in the socio-economic system that makes it difficult to ‘abruptly’ change trends. Conditions 3) and
 651 4) imply that CO₂-fe emissions are zero when the target is reached and stay zero afterward in the absence
 652 of any trend change in emissions. These boundary conditions leave two free parameters t_{target} and η . For
 653 each combination of these two parameters one emission curve exists. The maximum length of the time

654 series (t_{max}) varies dynamically depending on the REB and the CO₂-fe emissions in the year of the
655 stocktake:

656

$$657 \quad t_{max} = 30yr + 90yr \times e^{\left(\frac{|\max(REB-30 \text{ Pg C}, 0 \text{ Pg C})|}{50 \text{ Pg C}}\right)} + \min\left(|E_{fe}^{*CO_2}(t_{st})|, 10 \frac{\text{Pg C}}{\text{yr}}\right)^2 \times \frac{\text{yr}^3}{(\text{Pg C})^2}. \quad (6)$$

658

659 Each term in equation (6) is rounded to its nearest integer. This dynamic definition keeps the time until
660 which the temperature target should be reached (t_{max}) relatively short (close to 30 years, first term in
661 equation (6)) so that the temperature does not remain off target for too long. However, in two cases, it is
662 preferable that the REB is distributed over a longer time. The first case occurs when the anthropogenic
663 warming is close to the temperature target. In that case, a short t_{max} leads to abrupt short-term changes
664 in CO₂-fe emissions because a small REB (< ~100 Pg C) is forced into a small number of years
665 (Supplementary Figure 1). To avoid such an oscillation, t_{max} increases by up to additional 90 years when
666 the REB becomes small (term 2 in equation (6)). The second case occurs when the REB is large, but annual
667 emissions are still high (> ~5 Pg C yr⁻¹). These high emissions will already be correcting the temperatures
668 over time. A reduced t_{max} would force the large REB into a small number of years, and cause even higher
669 emissions in the first years, which need to be reduced shortly afterwards (Supplementary Figure 1). The
670 third term in equation (6), with $E_{fe}^{*CO_2}(t_{st})$ being equal to $E_{fe}^{CO_2}(t_{st})$ if the REB and $E_{fe}^{CO_2}(t_{st})$ have the
671 same sign and being zero otherwise, increases t_{max} by up to 100 years. Overall, the choice of the different
672 timescales does not rely on theoretical assumptions, but it is a result of tests across a wide range of
673 timescales.

674

675 For determining the free parameters t_{target} and η , we systematically varied them in steps of 1 year and 0.1
676 Pg C yr⁻² within the following limits: 5 years < ($t_{target}-t_{st}$) < t_{max} ; -2.5 Pg C yr⁻² < η < 2.5 Pg C yr⁻². The 'best'
677 choice out of these emission curves is chosen in three steps:

678 First, all curves are excluded whose integrated emissions from t_{st} to t_{target} do not agree with the REB within
679 ± 5 Pg C ($|\xi| < 5$ Pg C):

680

$$681 \quad \xi = \int_{t_{st}}^{t_{target}} E_{fe}^{CO_2}(t') dt' - REB, \quad (7)$$

682

683 with ξ being the difference between the REB and the integral of the CO₂-fe emission curve. In our tests,
684 at every stocktake at least one CO₂-fe emissions curve with a REB that lies within ± 5 Pg C of the REB
685 determined by the AERA is found. In the potential cases where a curve within the REB limit cannot be
686 found, the curve with the smallest $|\xi|$ would be chosen.

687

688 Second, among the remaining curves, all curves are excluded with exceedance emissions (ε) being larger
689 than 10 Pg C. Exceedance emissions are defined as follows:

690

$$691 \quad \int_{t_{st}}^{t_{target}} |E_{fe}^{CO_2}(t')| dt' - \int_{t_{st}}^{t_{target}} E_{fe}^{CO_2}(t') dt' < 2\varepsilon \quad (8)$$

692

693 The left side of equation (8) describes the difference between the integral of the absolute emissions over

694 time and the emissions integral. Although this difference is ideally zero, it can diverge if $E_{fe}^{CO_2}(t')$ changes

695 its sign between t_{st} and t_{target} . This can for example be the case if $E_{fe}^{CO_2}(t_{st})$ is still positive and $T_{ant}(t_{st})$ is

696 already larger than the temperature target. Thus, the still emitted positive emissions before emissions

697 become negative increase the exceedance of T_{ant} further and are therefore called 'exceedance emissions'.

698 They are later compensated by the roughly similar amount of negative emissions, hence the factor 2 on

699 the right side of equation (8). Several studies⁷⁷⁻⁸⁰ have shown that the global warming response to positive

700 and negative CO₂ emissions is indeed approximately symmetrical for moderate amounts of negative

701 emissions and under ambitious climate targets.

702 In 99.95% of the cases a CO₂-fe emissions curve with exceedance emissions smaller than 10 Pg C is found.
703 In the remaining 0.05% cases, the curve with the smallest exceedance emissions is chosen. In the 99.95%
704 of the cases where the limits for $|\xi|$ and exceedance emissions are met, the curve is retained with the
705 combination of t_{target} and η that results in the smallest curvature (sum of absolute changes in emissions
706 change). The smallest curvature is calculated by minimizing the sum of each curve's (absolute) second
707 derivatives from year t_{st-1} to year t_{target} .

708

709 CO₂-fe emissions from non-CO₂ agents

710

711 The historical CO₂-fe emissions from non-CO₂ agents are estimated based on the radiative forcing time-
712 series of non-CO₂ agents. This annual time series is translated into CO₂-fe emissions¹⁷:

713

$$714 \alpha E_{CO_2-fe}(t) = \frac{dF_{non-CO_2}(t)}{dt} + \rho F_{non-CO_2}(t), \quad (9)$$

715 with $F_{non-CO_2}(t)$ being the radiative forcing of non-CO₂ agents, $E_{CO_2-fe}(t)$ being CO₂-fe emissions from
716 non-CO₂ agents, with ρ being the rate of decline of radiative forcing over these timescales under zero
717 emissions (0.33%), and α being a constant representing the forcing impact of ongoing CO₂ emissions (1.08
718 W m⁻² per 1,000 GtCO₂).

719

720 Applying the AERA to observations until 2020

721

722 The necessary emission reductions in 2020 are quantified using the AERA. As input, we used the historical
723 GMST data from HadCRUT5 (<https://crudata.uea.ac.uk/cru/data/temperature/>), historical CO₂
724 concentrations from Meinshausen et al. (2017)⁸¹ until 2014 and from NOAA GML from 2015 to 2020
725 (https://gml.noaa.gov/webdata/ccgg/trends/co2/co2_annmean_gl.txt), historical radiative forcing from

726 non-CO₂ radiative agents from the RCP database, assuming RCP2.6 from 2005 to 2020
727 (<https://tntcat.iiasa.ac.at/RcpDb/dsd?Action=htmlpage&page=welcome>)⁸²⁻⁹⁰, historical CO₂ fossil fuel
728 and land-use change emissions from the Global Carbon Project³³, and historical CO₂-fe emissions from
729 non-CO₂ forcing agents derived from the non-CO₂ radiative forcing from the RCP database.

730

731 The estimated warming in 2020, past cumulative CO₂-fe emissions, and the remaining CO₂-fe emissions
732 budgets to limit global warming to 1.5°C and 2°C and the estimated time when zero CO₂-fe emissions need
733 to be reached based on this data lie within previous estimates. Previous estimates of the anthropogenic
734 warming are 1.0 ± 0.2°C in 2017², 1.07 (0.8-1.3)°C for the period from 2010-2019²⁹, and 1.20°C in 2020²⁶.
735 In comparison, the AERA-derived temperature is 1.15°C in 2017, 1.08°C from 2010 to 2019, and 1.23 in
736 2020, in agreement with the three previous estimates. The resulting remaining CO₂-fe budget, when
737 scaled to the remaining warming in 2020 (0.27°C), was estimated to be 117–270 Pg C^{7,21}. This estimation
738 encompasses the here presented REB estimate of 168 Pg C.

739

740 Supplementary Methods

741

742 Additional information about the methods that are used throughout this study is made available as
743 Supplementary Information. The Supplementary Information includes a detailed description of the AERA
744 testing with Bern3D-LPX, the reduced form atmospheric chemistry model, and the AERA robustness tests.

745

746

747 **References – Methods**

748

749 76. Millar, R. J., Nicholls, Z. R., Friedlingstein, P. & Allen, M. R. A modified impulse-response
750 representation of the global near-surface air temperature and atmospheric concentration
751 response to carbon dioxide emissions. *Atmos Chem Phys* **17**, 7213–7228 (2017).

752 77. Palter, J. B., Frölicher, T. L., Paynter, D. & John, J. G. Climate, ocean circulation, and sea
753 level changes under stabilization and overshoot pathways to 1.5K warming. *Earth System*
754 *Dynamics* **9**, 817–828 (2018).

755 78. Koven, C. *et al.* 23rd Century surprises: Long-term dynamics of the climate and carbon
756 cycle under both high and net negative emissions scenarios. *Earth System Dynamics*
757 *Discussions* **2021**, 1–32 (2021).

758 79. Zickfeld, K., MacDougall, A. H. & Matthews, H. D. On the proportionality between global
759 temperature change and cumulative CO₂ emissions during periods
760 of net negative CO₂ emissions. *Environmental Research Letters* **11**,
761 055006 (2016).

762 80. Tokarska, K. B., Zickfeld, K. & Rogelj, J. Path Independence of Carbon Budgets When
763 Meeting a Stringent Global Mean Temperature Target After an Overshoot. *Earths Future*
764 **7**, 1283–1295 (2019).

765 81. Meinshausen, M. *et al.* Historical greenhouse gas concentrations for climate modelling
766 (CMIP6). *Geosci Model Dev* **10**, 2057–2116 (2017).

767 82. van Vuuren, D. P. *et al.* Stabilizing greenhouse gas concentrations at low levels: an
768 assessment of reduction strategies and costs. *Clim Change* **81**, 119–159 (2007).

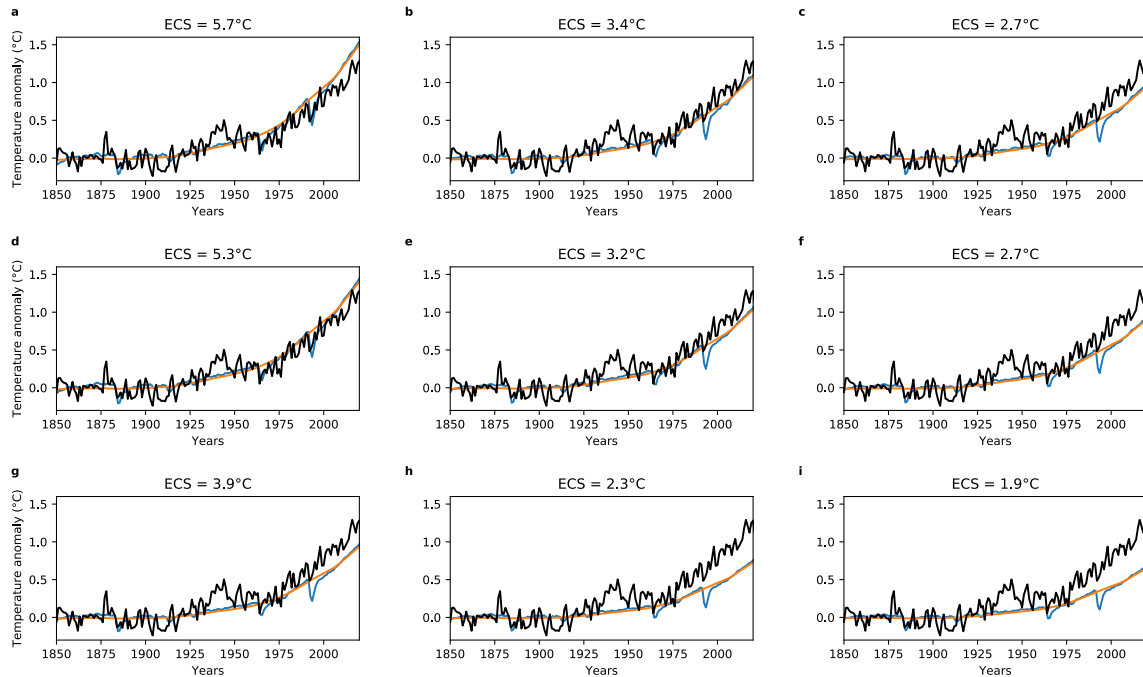
769 83. Schultz, M. G. *et al.* Global wildland fire emissions from 1960 to 2000. *Global Biogeochem*
770 *Cycles* **22**, (2008).

771 84. Mieville, A. *et al.* Emissions of gases and particles from biomass burning during the 20th
772 century using satellite data and an historical reconstruction. *Atmos Environ* **44**, 1469–1477
773 (2010).

774 85. Eyring, V. *et al.* Transport impacts on atmosphere and climate: Shipping. *Atmos Environ*
775 **44**, 4735–4771 (2010).

776 86. Lee, D. S. *et al.* Aviation and global climate change in the 21st century. *Atmos Environ* **43**,
777 3520–3537 (2009).

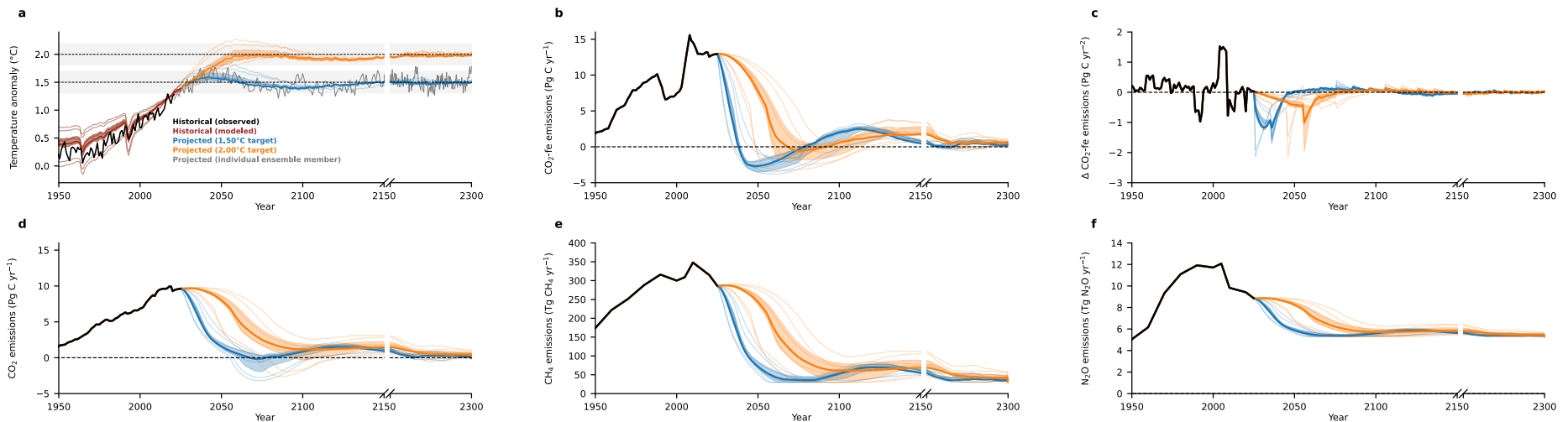
- 778 87. Lamarque, J.-F. *et al.* Historical (1850–2000) gridded anthropogenic and biomass burning
779 emissions of reactive gases and aerosols: methodology and application. *Atmos Chem Phys*
780 **10**, 7017–7039 (2010).
- 781 88. Hurtt, G. C. *et al.* Harmonization of land-use scenarios for the period 1500–2100:
782 600 years of global gridded annual land-use transitions, wood harvest, and resulting
783 secondary lands. *Clim Change* **109**, 117 (2011).
- 784 89. Smith, S. J., Pitcher, H. & Wigley, T. M. L. Global and regional anthropogenic sulfur dioxide
785 emissions. *Glob Planet Change* **29**, 99–119 (2001).
- 786 90. Bond, T. C. *et al.* Historical emissions of black and organic carbon aerosol from energy-
787 related combustion, 1850–2000. *Global Biogeochem Cycles* **21**, (2007).
- 788



789

790 **Extended Data Figure 1. Historical and simulated globally averaged surface atmospheric**
 791 **temperature anomaly with respect to 1850-1900 for different model configurations. (a-i) Global**
 792 **mean surface temperature (GMST) from 1850 to 2020 for 9 model configurations with varying ECS**
 793 **without the superimposed inter-annual variability. The blue lines show the simulated GMST, and the**
 794 **orange lines show the determined anthropogenic warming. The diapycnal diffusivity coefficients are**
 795 **1×10^{-5} , 2×10^{-5} and $1 \times 10^{-4} \text{ m}^2 \text{ s}^{-1}$ (from top to bottom) and the different numbers for the internal Bern3D**
 796 **model parameter that accounts for climate feedbacks, which are not explicitly represented in the**
 797 **model, are 0.1, -0.5, and $-0.8 \text{ W m}^{-2} \text{ K}^{-1}$ (from left to right). The HadCRUT5 observation-based GMST**
 798 **time-series is shown in black in all panels.**

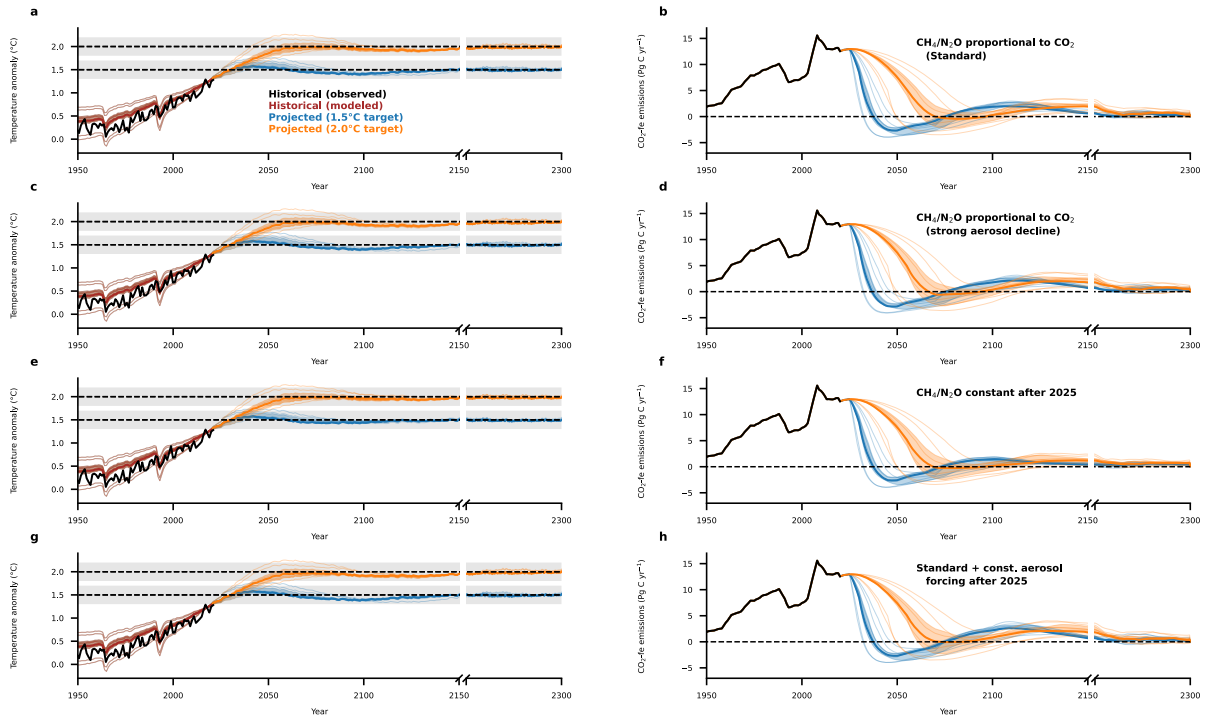
799



800

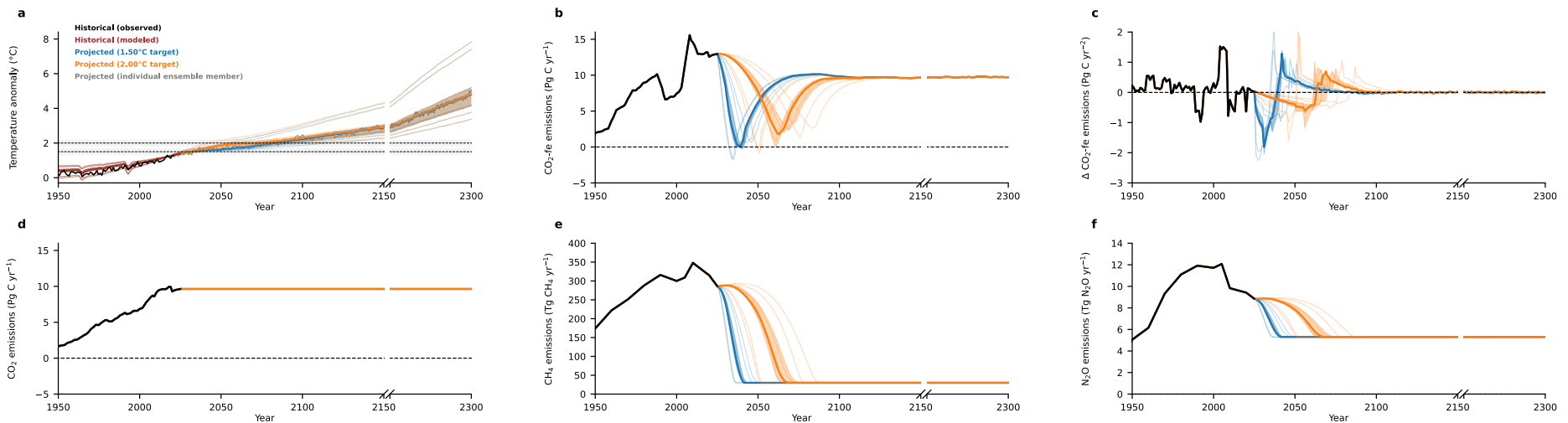
801 **Extended Data Figure 2. Globally averaged surface atmospheric temperature anomaly with respect to 1850-1900, CO₂-fe emissions, their annual rate of**
 802 **change, as well as CO₂, CH₄, and N₂O emissions when applying the adaptive emission reduction approach every ten years. (a)** Temperature anomalies with
 803 respect to 1850-1900, **(b)** CO₂-fe emissions, and **(c)** their annual rate of change if the AERA is applied every ten years starting in the year 2025 for the 1.5°C
 804 target (blue) and the 2.0°C target (orange). In addition, the AERA-calculated emission curves for **(d)** CO₂, **(e)** CH₄, and **(f)** N₂O are shown. As compared to figure
 805 2 in the main text, here the CO₂ emissions are forced to remain constant while only CH₄, N₂O, VOC, NO_x, and CO emissions evolve proportionally. The thick
 806 solid lines show the average of the 8 simulations with varying magnitude and timing of added inter-annual temperature variability of the Bern3D-LPX model
 807 configuration with an ECS of 3.2°C, the thin solid lines show the same for the remaining 8 configurations covering ECS from 1.9 to 5.7°C, and the shaded area
 808 shows the range of all configurations that fall within the likely range of ECS as defined by Sherwood et al. (2020)¹⁷. The grey shading in **(a)** indicates the
 809 uncertainty with which the anthropogenic warming can be determined ($\pm 0.2^\circ\text{C}$)⁵³⁻⁵⁶.

810



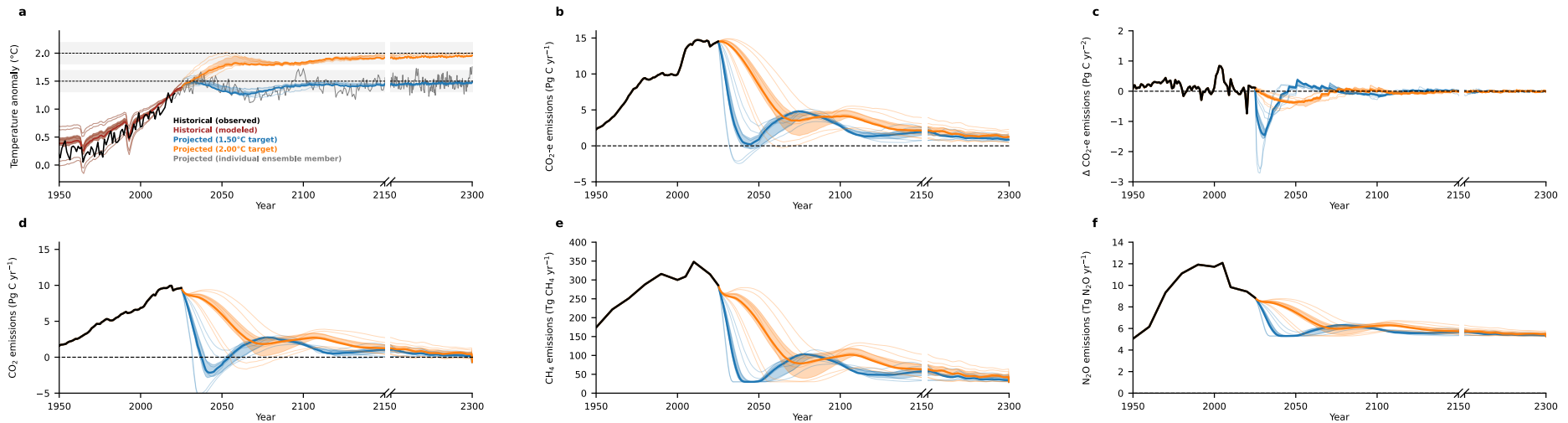
811

812 **Extended Data Figure 3. Adaptive CO₂-fe emissions and resulting temperature anomaly for 1.5°C and**
 813 **2.0°C target for different non-CO₂ GHG emissions and aerosol radiative forcing. (a, c, e, g)**
 814 Temperature anomalies with respect to 1850-1900 and **(b, d, f, h)** corresponding CO₂-fe emissions if
 815 the AERA is applied every five years starting in the year 2025 for the 1.5°C target (blue) and the 2.0°C
 816 target (orange) for four different idealized cases: **(a, b)** aerosol radiative forcing decreases
 817 exponentially and CO₂, CH₄, and N₂O emissions evolve proportionally, **(c, d)** aerosol radiative forcing
 818 decreases according to the CO₂ emissions and CO₂, CH₄, and N₂O emissions evolve proportionally, **(e,**
 819 **f)** aerosol radiative forcing decreases exponentially but CH₄, and N₂O emissions remain constant after
 820 2025 and only CO₂ evolves dynamically, and **(g, h)** aerosol radiative forcing remains constant after 2025
 821 and CO₂, CH₄, and N₂O emissions evolve proportionally. The thick solid lines show the average of the 8
 822 simulations with varying magnitude and timing of added inter-annual temperature variability of the
 823 Bern3D-LPX model configuration with an ECS of 3.2°C and the shaded area shows the range of all
 824 configurations that fall within the likely range of ECS as defined by Sherwood et al. (2020)¹⁷. The grey
 825 shading in **(a, c, e, g)** indicates the uncertainty with which the anthropogenic warming can be
 826 determined ($\pm 0.2^\circ\text{C}$)⁵³⁻⁵⁶. The corresponding CO₂, CH₄, and N₂O emissions and aerosol forcing for each
 827 simulated case are shown in Figure 3.



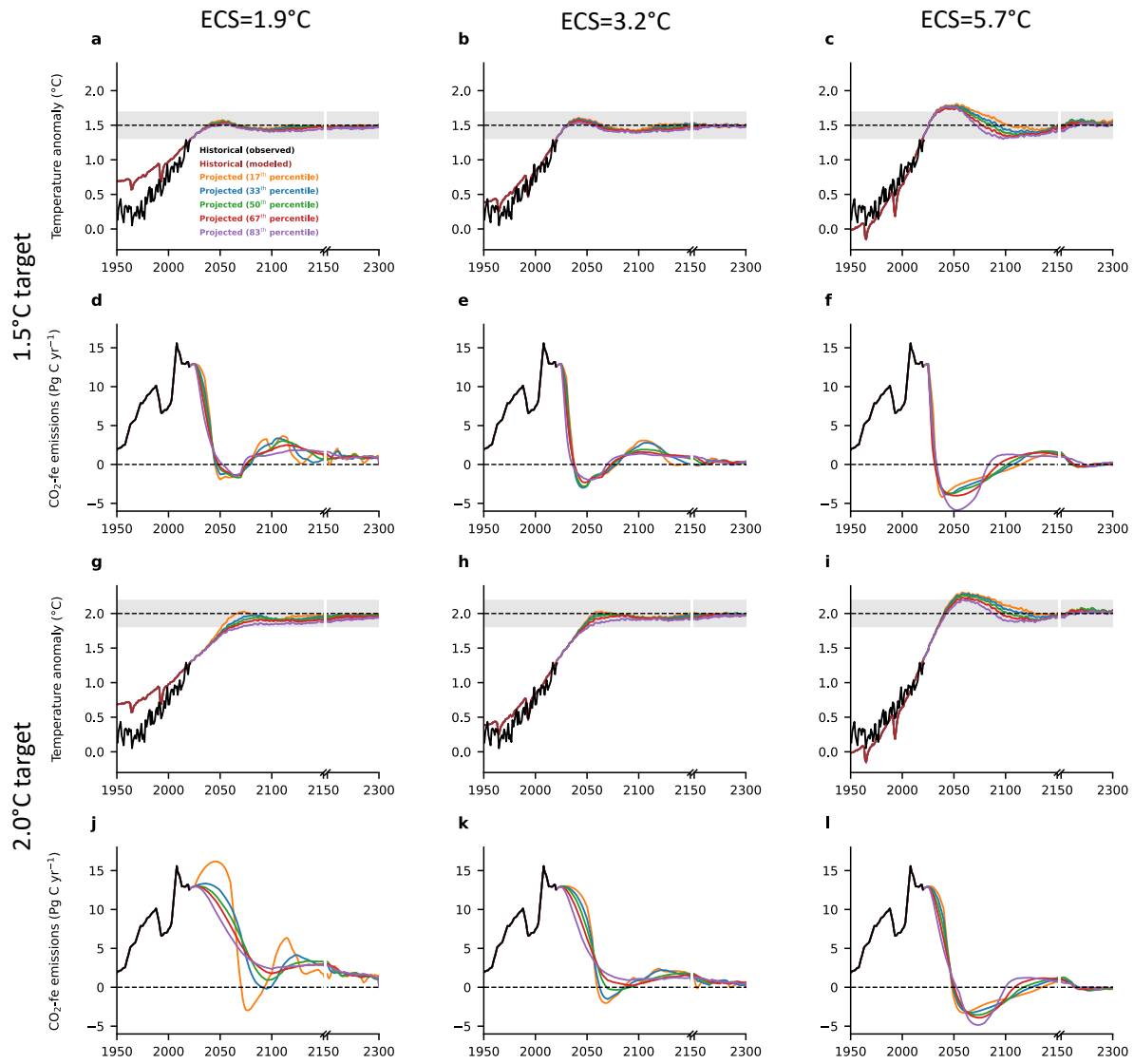
828

829 **Extended Data Figure 4. Globally averaged surface atmospheric temperature anomaly with respect to 1850-1900, CO₂-fe emissions, their annual rate of**
 830 **change, as well as CO₂, CH₄, and N₂O emissions following the adaptive emission reduction approach when forcing CO₂ emissions to remain constant. (a)**
 831 **Temperature anomalies with respect to 1850-1900, (b) CO₂-fe emissions, and (c) their annual rate of change if the AERA is applied every five years starting in**
 832 **the year 2025 for the 1.5°C target (blue) and the 2.0°C target (orange). In addition, the AERA-calculated emission curves for (d) CO₂, (e) CH₄, and (f) N₂O are**
 833 **shown. As compared to figure 2 in the main text, here the CO₂ emissions are forced to remain constant while only CH₄, N₂O, VOC, NO_x, and CO emissions**
 834 **evolve proportionally. The thick solid lines show the average of the 8 simulations with varying magnitude and timing of added inter-annual temperature**
 835 **variability of the Bern3D-LPX model configuration with an ECS of 3.2°C, the thin solid lines show the same for the remaining 8 configurations covering ECS**
 836 **from 1.9 to 5.7°C, and the shaded area shows the range of all configurations that fall within the likely range of ECS as defined by Sherwood et al. (2020)¹⁷. The**
 837 **grey shading in (a) indicates the uncertainty with which the anthropogenic warming can be determined ($\pm 0.2^\circ\text{C}$)⁵³⁻⁵⁶.**



838

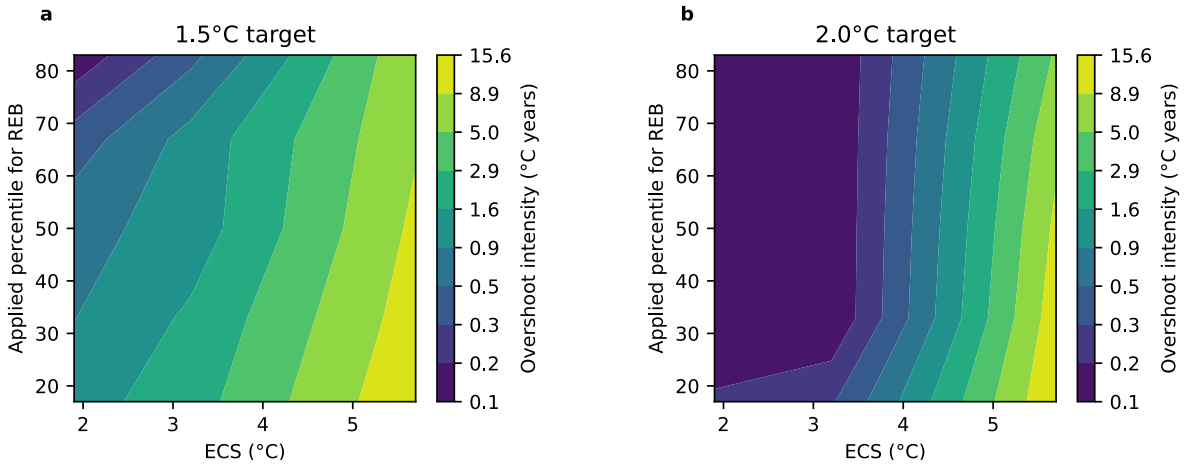
839 **Extended Data Figure 5. Globally averaged surface atmospheric temperature anomaly with respect to 1850-1900, CO₂-e emissions, their annual rate of**
 840 **change, as well as CO₂, CH₄, and N₂O emissions following the adaptive emission reduction approach using GWP-100 instead of CO₂-fe to split CO₂-e**
 841 **emissions. (a) Temperature anomalies with respect to 1850-1900, (b) CO₂-e emissions, and (c) their annual rate of change if the AERA is applied every five**
 842 **years starting in the year 2025 for the 1.5°C target (blue) and the 2.0°C target (orange). In addition, the AERA-calculated emission curves for (d) CO₂, (e) CH₄,**
 843 **and (f) N₂O are shown. As compared to figure 2 in the main text, here the GWP-100 approach was used to calculate CO₂ equivalent emissions from CH₄ and**
 844 **N₂O emissions and the CO₂-fe emissions approach was applied to calculate CO₂ equivalent emissions from the remaining forcing agents. The thick solid lines**
 845 **show the average of the 8 simulations with varying magnitude and timing of added inter-annual temperature variability of the Bern3D-LPX model configuration**
 846 **with an ECS of 3.2°C, the thin solid lines show the same for the remaining 8 configurations covering ECS from 1.9 to 5.7°C, and the shaded area shows the**
 847 **range of all configurations that fall within the likely range of ECS as defined by Sherwood et al. (2020)¹⁷. The grey shading in (a) indicates the uncertainty with**
 848 **which the anthropogenic warming can be determined ($\pm 0.2^\circ\text{C}$)⁵³⁻⁵⁶**



849

850 **Extended Data Figure 6. Adaptive emissions and resulting temperature anomaly for 1.5°C and 2.0°C**
 851 **target with varying compliance.** Temperature from 2020 to 2300 for three model configurations with
 852 varying ECS (1.9°C (a, d, g, j), 3.2°C (b, e, h, k), 5.7°C (c, f, i, l)) averaged over four simulations each with
 853 different inter-annual variability for the (a-c) 1.5°C and (g-i) 2.0°C temperature target and (d-f, j-l) the
 854 respective CO₂-fe emission curves with different compliance, i.e., at each stocktake the 17th (orange), 33rd
 855 (blue), 50th (green), 67th (red), or 83rd percentile (violet) was implemented. The percentiles are scaled at
 856 each stocktake based on the percentiles of the REB in 2020 from Table 5.8 of the IPCC AR6 WG1 report⁸⁹.
 857 The grey shading in (a, b, c, g, h, i) indicates the uncertainty with which the anthropogenic warming can
 858 be determined ($\pm 0.2^\circ\text{C}$)^{53–56}.

859



860

861 **Extended Data Figure 7. Overshoot cumulative intensity for 1.5°C and 2°C temperature targets**
 862 **dependent on compliance and model configuration.** Overshoot cumulative intensity (°C years), defined
 863 as the sum of the overshoot temperatures in each year, in dependence of model configuration (ECS from
 864 1.9°C to 5.7°C) and the REB that was used in the AERA (17th, 33rd, 50th, 67th, and 83rd percentile) for **(a)**
 865 1.5°C and **(b)** 2°C target.

Supplementary Information

Testing the AERA with Bern3D-LPX

The AERA was tested using the Bern3D-LPX model, version 2.0^{62,63} with nine model configurations with combinations of three ocean diapycnal mixing coefficients ($1e^{-4}$, $2e^{-5}$, $1e^{-5}$ $m^2 s^{-1}$) and three temperature sensitivities to radiative forcing. These three sensitivities to radiative forcing are created by varying an internal Bern3D model parameter that accounts for climate feedbacks, which are not explicitly represented in the model (-0.7 , -0.3 , 0.1 $W m^{-2} K^{-1}$). These nine configurations cover the ECS range from 1.9 to 5.7 °C and the TCR range from 1.3 to 2.5 °C. This range represents the range of TCR/ECS estimates based on multiple lines of evidence²⁴.

For each configuration, the same set of simulations were performed. In these simulations, land-use change CO₂ emissions were interactively simulated by the biosphere component of the Bern3D-LPX model⁶³ by prescribing land-use area. More specifically, over the historical 1750-2014 period, historical land-use area was prescribed⁹¹. From 2015 to 2100, land-use area was assumed to follow the low-emissions pathway SSP1-2.6, and from 2100 to 2300 land-use area was assumed to be constant. The corresponding land-use change CO₂ emissions were diagnosed by the difference in air-land CO₂ flux between a simulation with constant land-use area and one with changing land use as prescribed above. Both simulations had the same atmospheric CO₂ concentrations, following historical records until 2014 and SSP1-2.6 afterward⁸¹. Historical non-CO₂ radiative forcing from 1850 to 2004 was prescribed by values from the RCP database (<https://tntcat.iiasa.ac.at/RcpDb/dsd?Action=htmlpage&page=welcome>)^{83-90,92}, and non-CO₂ radiative forcing from 2005 to 2025 follows the SSP1-2.6 scenario as described in the SSP database (<https://tntcat.iiasa.ac.at/SspDb/dsd?Action=htmlpage&page=10>)^{93,94}. After 2025, the non-CO₂ radiative forcing was either develop dynamically depending on the AERA-prescribed CO₂-fe emissions or was prescribed as a time-series. Before 1850, the non-CO₂ radiative forcing is held

constant at the values from 1850. Historical fossil fuel CO₂ emissions are prescribed from 1765 to 2019 based on the Global Carbon Project³³, and in 2020 based on Le Quéré et al. (2021)⁹⁵. Prescribed fossil fuel CO₂ emissions from 2021 to 2025 are assumed to evolve proportionally to the estimated CO₂-fe emissions that were estimated from the Nationally Determined Contributions (NDC) (Climate Action Tracker⁶⁵).

The different ECSs in each configuration lead to a range of $\Delta T_{ant}^{model}(2020)$ of 0.64 to 1.48°C. Due to this difference, ΔT_{ant}^{target} is defined for each configuration so that $\Delta T_{ant}^{target} - \Delta T_{ant}^{model}(2020)$ equals the $\Delta T_{ant}^{target} - \Delta T_{ant}^{obs}(2020)$ calculated from observations. Thus, for each model configuration the remaining warming from 2020 onwards is the same and differences in the emission curves after 2020 result solely from the differences in ocean mixing and temperature sensitivity and not from differences in the already realized model warming. The historical $\Delta T_{ant}(2020)$ calculated as described above is 1.23°C, leaving an allowable warming of 0.27°C for the 1.5°C target and 0.77°C for the 2°C target.

From 2025 onward, CO₂-fe emissions are calculated by the AERA every 5 years starting in 2025 to mimic the global stocktake process (UNFCCC 2015⁶). For the first step of the AERA, the historical time-series of temperature and RF are needed to calculate the anthropogenic warming at the time of the stocktake. The historical temperature timeseries is directly taken from the simulated model output for each configuration. In addition, an artificial temperature anomaly was added to the simulated temperature in Bern3D, as the modelled inter-annual variability is strongly underestimated. The added anomaly is derived from observed GMST (HadCRUT5) from 1920 to 2019 by subtracting a 3rd order polynomial fit. This 100-year time series is added periodically. To create different anomalies, the anomaly was also added with different phasing (25, 50, and 75 years) and also with a changing sign, resulting in 8 different temperature time series for each model configuration. The past RF is a combination of the CO₂ and non-CO₂. The non-CO₂ RF is directly taken from the prescribed RF to Bern3D-LPX. The CO₂ RF is calculated following IPCC AR6, Table 7.SM.1⁹⁶ using the dynamically

simulated atmospheric CO₂ in the respective simulation and prescribed atmospheric N₂O based on the RCP and SSP databases following SSP1-2.6. In the second step, the REB is estimated based on the anthropogenic warming from step one and the past CO₂-fe emission curve. The past CO₂-fe emission curve is the sum of the dynamically adapted fossil fuel CO₂ emissions, the emissions from prescribed land-use area (smoothed with a 21-year running mean due to its relatively large inter-annual variability), and the non-CO₂ forcing agent emissions that are derived from the prescribed non-CO₂ radiative forcing (smoothed with a 5-year running mean to avoid artificially steps in the emissions that arise from the radiative forcing data that is only provided every 10 years). The CO₂ equivalent emissions from non-CO₂ forcing agents are derived from the prescribed non-CO₂ radiative forcing using the CO₂-fe emissions approach¹⁷. In the last step of the AERA, the REB is distributed over the following years. In the standard case, the CO₂ equivalent emissions are split using the CO₂-fe emissions approach¹⁷. When testing the AERA with the GWP-100 approach (Extended Data Figure 5), the equivalent CO₂ emissions from CH₄ and N₂O emissions for the period after the stocktake are calculated using GWP-100, while the CO₂-fe emissions approach is used to transfer the radiative forcing from the remaining non-CO₂ forcing agents (aerosols, halogens, ...). The effect of CH₄ on tropospheric ozone is accounted for by GWP-100 and only the remaining radiative forcing by ozone, which is mainly caused by CO, VOC, and NO_x, and to a small extent by stratospheric ozone, is transferred via the CO₂-fe emissions approach (Supplementary Figure 2).

After the AERA is applied, the future adapted CO₂-fe emission curve is again divided into different components (CO₂ fossil fuel emissions, land use change CO₂ emissions, non-CO₂ emissions). First, the prescribed land-use change CO₂ emissions are subtracted from the CO₂-fe emission curve that was determined from the AERA. The radiative forcing and CO₂-fe emissions from non-CO₂ radiative agents are calculated using a reduced form atmospheric chemistry model⁶⁴ updated with the latest information from IPCC AR6. The reduced form atmospheric chemistry model takes time series of CH₄, N₂O, CO, VOC, and NO_x emissions, as well as time series of radiative forcing of aerosols and halogens,

as input to calculate future fossil fuel CO₂ emissions and the radiative forcing from non-CO₂ radiative agents from which the corresponding non-CO₂ CO₂-fe emissions are calculated. In the standard case (Figure 2), CO₂, CH₄ and, N₂O emissions after 2025 evolve proportionally and are chosen so that fossil fuel CO₂ emissions and CO₂-fe emissions from non-CO₂ radiative agents fit the prescribed CO₂-fe emissions by the AERA (minus the land use change CO₂ emissions). However, CH₄, and N₂O emissions cannot descend below the thresholds 30 Tg CH₄ yr⁻¹ and 5.3 Tg N₂O yr⁻¹, respectively, due to the difficulty in abating CH₄ and N₂O emissions from agricultural and livestock sectors. The N₂O emissions threshold is chosen as the minimum N₂O emissions across the 21st century and across the range of SSPs from the SSP database. The minimum CH₄ emissions prescribed here are below the minimum CH₄ across all SSPs and present the most optimistic future for possible CH₄ reductions. Recent estimates quantify the potential reduction in CH₄ emissions until 2030 to be 45-54% (Emissions Gap Report 2021⁹⁷ and the Global Methane Initiative (<https://www.globalmethane.org/documents/gmi-mitigation-factsheet.pdf>)). Here, we assumed that 45% is possible until 2030 and another 45% is possible until 2300. While this is clearly optimistic, large-scale negative CO₂ emissions are also optimistic. In alternative cases (Figure 3 & Extended Data Figure 3), CH₄ and N₂O emissions after 2025 are prescribed and only fossil fuel CO₂ emissions after 2025 are dynamically chosen so that fossil fuel CO₂ emissions and CO₂-fe emissions from non-CO₂ radiative agents fit the prescribed CO₂-fe emissions by the AERA (minus the land use change CO₂ emissions) (Supplementary Figure 2).

Reduced form atmospheric chemistry model

The reduced form atmospheric chemistry model calculates the effective radiative forcing for non-CO₂ radiative forcing agents based on prescribed emissions, as well as time series of radiative forcing of aerosols and halogens⁶⁴ with updated equations and constants. The reduced chemistry model is initialized in 2019 from observational data and evolves over time as follows:

- Anthropogenic CH₄ and, N₂O emissions are prescribed as input.

- Natural CH₄ and, N₂O emissions are supposed to be constant over time and are set to 218 Tg CH₄ yr⁻¹ and 9.7 Tg N yr⁻¹, respectively. Natural N₂O emissions are taken from Tian et al. (2020)³⁶ and natural CH₄ emissions are calculated from the change in atmospheric CH₄ mixing ratio from 2000 to 2017 from NOAA (https://gml.noaa.gov/ccgg/trends_ch4/), anthropogenic CH₄ emissions from 2000 to 2017 from the Global Methane Budget³¹, and an atmospheric lifetime CH₄ of 9.1 years (based on Tab 6.2 IPCC AR6 and associated text)⁹⁸.
- CO, VOC, and NO_x emissions in 2019 are initialized based on the respective emissions in 2020 in the SSP database following SSP1-2.6 (763.5 Tg CO yr⁻¹; 128.6 Tg VOC yr⁻¹; 123.6 Tg NO₂ yr⁻¹). After 2019, these CO, VOC, and NO_x emissions are assumed for simplicity to evolve proportional to CO₂ emissions, although these emissions are linked to a range of sources such as fossil fuel burning, N-fertilizer use, or biomass burning and their relationship with CO₂ emissions may change through time. These emissions are assumed to not be able to drop below their respective emissions in 2100 following SSP1-2.6: 307.2 Tg CO yr⁻¹; 38.4 Tg VOC yr⁻¹; 32.4 Tg NO₂ yr⁻¹.
- Preindustrial and 2019 atmospheric mole fractions of CH₄ (731.41 and 1825.00 ppb) and N₂O (273.87 and 330.50 ppb) are prescribed based on tables 7.5 and 7.SM.1 and chapter 7 of IPCC AR6⁹⁶. After 2019, atmospheric mole fractions of CH₄ and N₂O evolve dynamically as explained below.
- CH₄ mole fraction is calculated forward every year as follows:

$$CH_4(t+1) = CH_4(t) + \frac{ppb}{2.75 \text{ Tg } CH_4} \left(E_{nat}^{CH_4}(t+1) + E_{ant}^{CH_4}(t+1) \right) - \frac{CH_4(t)}{\tau_{CH_4(t)}},$$

(10)

with $CH_4(t)$ being the CH₄ mole fraction (ppb) in year t , $E_{nat}^{CH_4}$ being the natural CH₄ emissions (Tg CH₄), $E_{ant}^{CH_4}$ being the anthropogenic CH₄ emissions (Tg CH₄), $\frac{ppb}{2.75 \text{ Tg } CH_4}$ being the conversion

factor from the IPCC AR6 report⁹⁹, and $\tau_{CH_4}(t)$ being the life time of CH₄ (yr) that is calculated as follows:

$$\tau_{CH_4}(t) = \left(\frac{rOH}{11yr} + \frac{1}{52.4 yr} \right)^{-1}, \quad (11)$$

with lifetimes based on Tab 6.2 in IPCC AR6 Chapter 6⁹⁶ and Prather et al. (2012)¹⁰⁰ and rOH being the relative change in tropospheric OH with respect to year 2019:

$$\ln(rOH) = \ln \left(\frac{OH(t)}{OH(2019)} \right) = -0.32 * \ln \left(\frac{CH_4(t)}{CH_4(2019)} \right) + 0.0042 * \left(\frac{E_{NO_x}(t)}{E_{NO_x}(2019)} \right) - 0.000105 * \left(\frac{E_{CO}(t)}{E_{CO}(2019)} \right) - 0.000313 * \left(\frac{E_{VOC}(t)}{E_{VOC}(2019)} \right), \quad (12)$$

with $E_{NO_x}(t)$, $E_{CO}(t)$, and $E_{VOC}(t)$ being the emissions from CO, VOC, and NO_x.

- N₂O concentrations change is calculated forward every year as follows:

$$N_2O(t+1) = N_2O(t) + \frac{ppb}{4.79 Tg N} \left(E_{nat}^{N_2O}(t+1) + E_{ant}^{N_2O}(t+1) \right) - \frac{N_2O(t)}{\tau_{N_2O}(t)} yr, \quad (13)$$

with $N_2O(t)$ being the N₂O concentrations (ppb) in year t , $E_{nat}^{N_2O}$ being the natural N₂O emissions (Tg N), $E_{ant}^{N_2O}$ being the anthropogenic N₂O emissions (Tg N), $\frac{ppb}{4.79 Tg N}$ being the conversion factor from Prather et al. (2012)¹⁰⁰, and $\tau_{N_2O}(t)$ being the lifetime of N₂O (yr)⁶⁴:

$$\tau_{N_2O}(t) = 116 yr * \left(\frac{E_{ant}^{N_2O}(t)}{E_{ant}^{N_2O}(2019)} \right)^{-0.055}, \quad (14)$$

with the mean lifetime (116 years) being based on chapter 5 of IPCC AR6⁹⁶.

- The stratospheric adjusted radiative forcing for CH₄ and N₂O is calculated as described in chapter 7 of IPCC AR6, Table 7.SM.1⁹⁶. From that, the effective radiative forcing is calculated using adjustment factors (0.86 for CH₄ and 1.07 for N₂O) from chapter 7 of IPCC AR6⁹⁶.
- Effective radiative forcing of tropospheric O₃ in 2019 is set to 0.34 W m⁻² and evolves over time as described in equation 7.SM.1.3 in IPCC AR6 CH7⁹⁶. The effective radiative forcing of tropospheric O₃ in 2019 is within the uncertainty range given in Figure 7.6 in IPCC AR6 CH7⁹⁶. Although the best estimate is 0.47 W m⁻², we have reduced the effective radiative forcing so that the total non-CO₂ radiative forcing in 2025 that is estimated by the reduced atmospheric chemistry model is consistent with the prescribed non-CO₂ radiative forcing in Bern3D based on the RCP and SSP databases following SSP1-2.6 that was used until 2025. The effective radiative forcing of stratospheric O₃ is of the order of -0.05 W m⁻² and included in the remaining effective radiative forcing (see below).
- Total halogen effective forcing radiative forcing in 2019 is set to 0.41 W m⁻² (Figure 7.6 in IPCC AR6 CH7⁹⁶) is divided into short-lived halogens with a lifetime of 12 years (0.08 W m⁻²), medium-lived halogens with a lifetime of 40 years (0.09 W m⁻²), long-lived halogens with a lifetime of 100 years (0.21 W m⁻²), and 'eternal' halogens (0.03 W m⁻²) based on table 7.SM.1.3 in IPCC AR6 CH7⁹⁶. The halogen radiative forcing is assumed to decay depending on the lifetime with no source of halogens.
- The aerosol effective radiative forcing is set to -1.1 W m⁻² in 2019 following Figure 7.6 in IPCC AR6 Chapter 7⁹⁶. After 2019, the aerosol forcing decays exponentially in the standard case. Half of it is assumed to decline with a half-life of 20 years and half is assumed to decay with a half-life of 250 years to approximate an aerosol forcing that co-evolves with the strong reductions in CO₂ emissions that need to be achieved to limit warming to temperatures between 1.5°C and 2°C.

- Effective radiative forcing of stratospheric water vapor ($ERF_{H_2O}(t)$) is calculated based on the atmospheric CH_4 mixing ratio in the respective year ($CH_4(t)$) and the preindustrial atmospheric CH_4 mixing ratio (CH_4^{pi})⁶⁴:

$$ERF_{H_2O}(t) = \alpha_{H_2O} \left(\sqrt{CH_4(t)} - \sqrt{CH_4^{pi}} \right),$$

(15)

With α_{H_2O} set to $0.0031 \frac{W}{m^2 \text{ ppb}^{\frac{1}{2}}}$ so that $ERF_{H_2O}(2019)$ is $0.05 \frac{W}{m^2}$ as in Figure 7.6 in IPCC AR6

Chapter 7⁹⁶.

- Remaining effective radiative forcing (albedo, stratospheric O_3 , contrails, ...) is for simplicity assumed to stay constant at -0.07 W m^{-2} based on Figure 7.6 in IPCC AR6 CH7⁹⁶.

AERA robustness tests

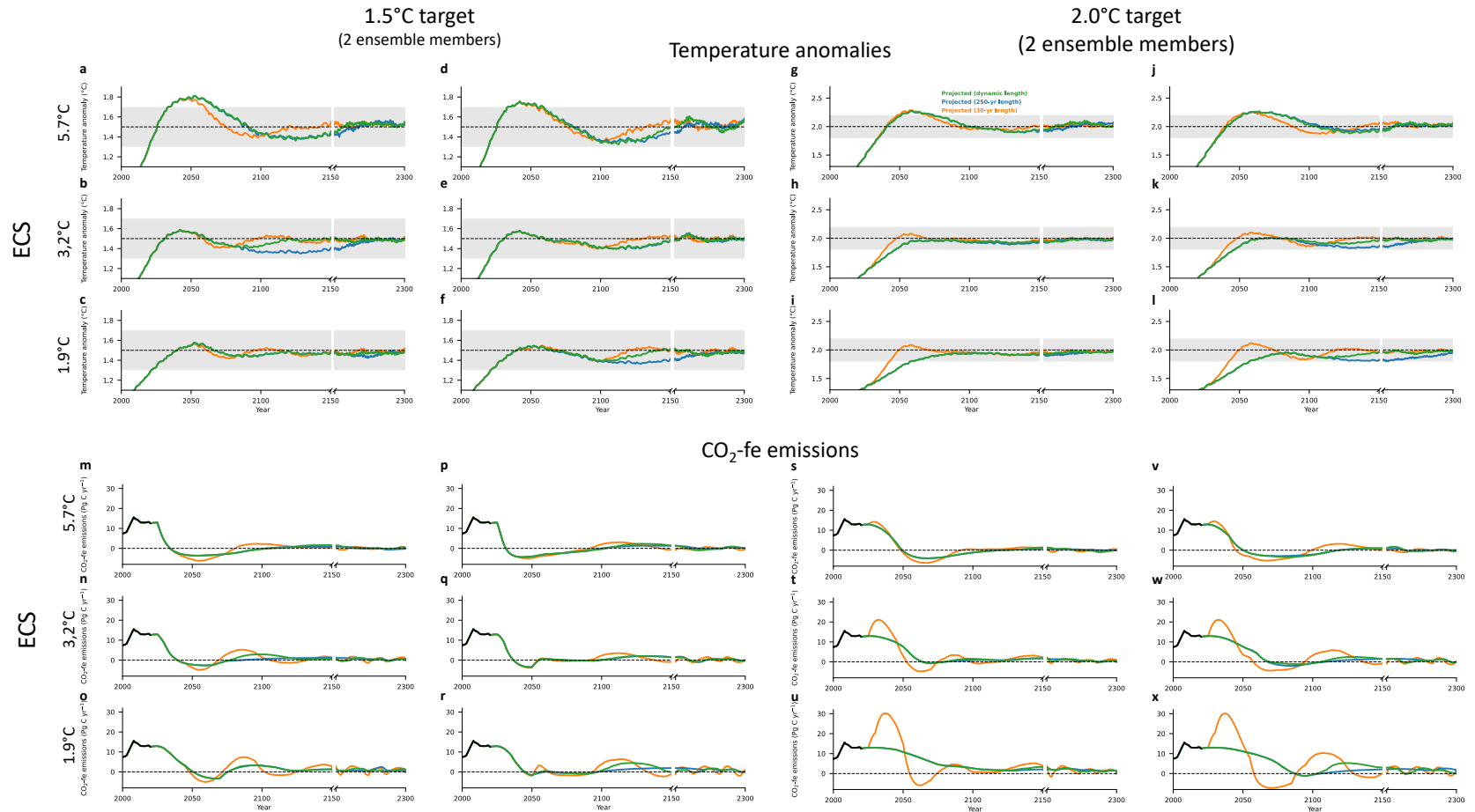
The AERA was tested for robustness within the Bern3D-LPX model framework. These tests are made with the standard version (CO_2 -fe approach and CO_2 , CH_4 , and N_2O emissions evolving proportional after 2025) and include varying the allowed difference to the REB (ξ) and the allowed integrated exceedance emissions (ε) when fitting the future total CO_2 -fe emissions curve, and testing the algorithm when Bern3D has been used with different non- CO_2 GHG radiative forcing than that 'seen' by the AERA to ensure that the AERA still works even if the past radiative forcing estimates are incorrect.

The sensitivities towards the allowed difference to the REB (ξ) and the allowed exceedance emissions (ε) were tested with three model configurations (ECS=1.9°C, 3.2°C, 5.7°C) with 4 instead of 8 different temperature anomalies superimposed in each case for computational reasons. Simulations were made

with half and twice the amount of ξ and ε . CO₂-fe emissions from 2025 to 2300 are on average not different from the standard version when ξ is halved or doubled (0.0 ± 0.1 Pg C yr⁻¹), but minimum CO₂-fe emissions in the 21st century are marginally less pronounced if ξ is halved and more pronounced if ξ is doubled (Supplementary Figure 3). The temperature curves are also indifferent. When exceedance emissions are halved, temperature curves remain almost unchanged, whereas CO₂-fe emissions become less smooth when the temperature anomaly is close to the temperature target (Supplementary Figure 4). In such a situation, a fast change in the sign of the REB between two stocktakes due to natural variability in the temperature likely causes the abrupt changes in the CO₂-fe emissions curve. When ε is doubled, the temperature overshoot in the 21st century becomes larger for the high ECS configuration by up to 0.06°C but leaves temperature curves for the other configurations unchanged. In return, the CO₂-fe emissions curves become slightly smoother. Overall, the chosen best parameters for ξ and ε present the best compromise between the smoothness of the emission curves and the degree of a temperature overshoot.

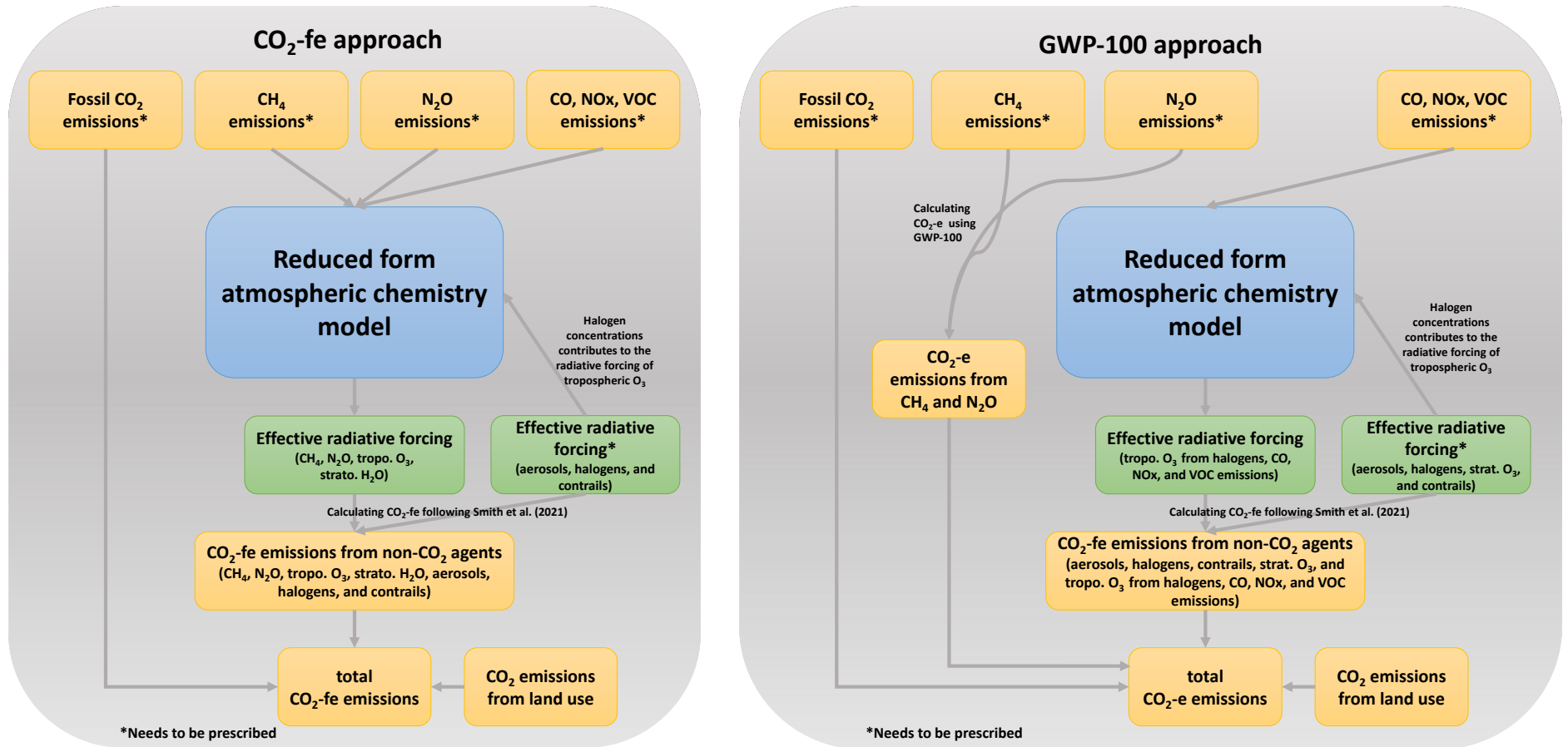
To test the robustness of the AERA towards the estimate of the past radiative forcing, the radiative forcing from aerosols was adjusted in the model, whereas the non-CO₂ radiative forcing and the corresponding CO₂-fe that are 'seen' by the AERA are not adjusted. The radiative forcing of aerosols in 2011 was taken from the central estimate of the IPCC report WG1 2013⁵⁹. It was extrapolated back and forward (until 2025) in time using sulfur emissions as a proxy from the RCP and SSP databases. After 2025, the radiative forcing is calculated by the reduced form chemistry model. Once the aerosol radiative forcing time series is determined, this timeseries of aerosol forcing was adjusted by $\pm 40\%$. The model was then run with 3 different configurations (ECS = 1.9, 3.2 and 5.7°C). However, only a few combinations of ECS and adjusted aerosol forcing are credible, i.e., a small aerosol forcing in combination with a large ECS results in too strong warming over the historical period whereas a small ECS and a large cooling aerosol forcing results in almost no temperature rise over the same period. We then chose the combinations that represent the historical warming best: low ECS and low aerosol

forcing and high ECS and high aerosol forcing (Supplementary Figure 5). Overall, the AERA still works in both cases. If aerosol forcing is less strong than expected, a reduction of aerosols does not cause the expected warming and emissions reductions can be less pronounced. However, if aerosol forcing is underestimated, a reduction of aerosols over the 21st century will cause pronounced warming and an overshoot of 0.58°C to which the AERA reacts with strong emissions reductions. The AERA thus automatically corrects the underestimation of the aerosol forcing.



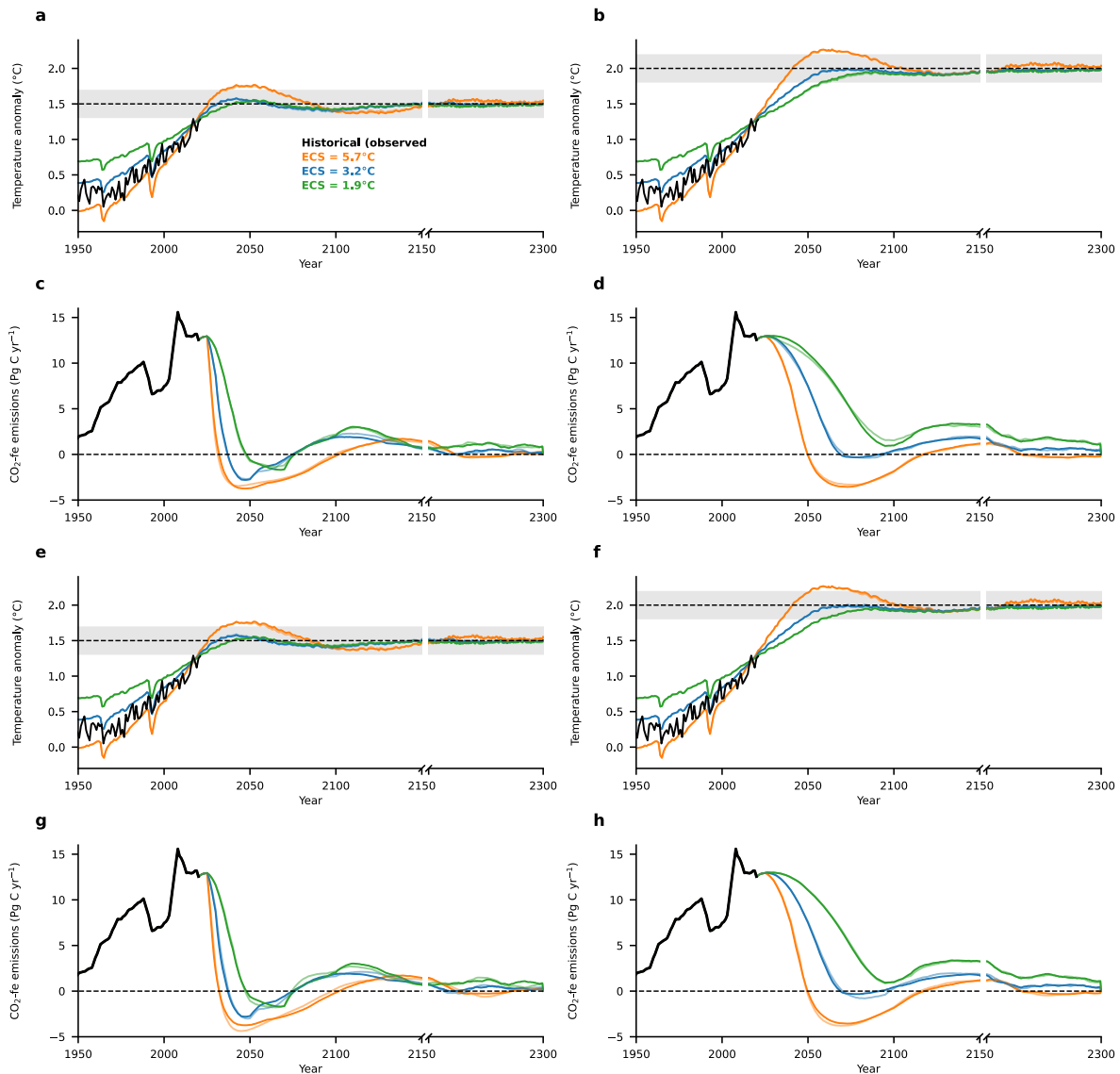
Supplementary Figure 1. Sensitivity of results to maximum length of the prescribed polynomial function in the AERA algorithm. (a-l) Temperature anomalies with respect to 1850-1900 and **(m-x)** corresponding CO₂-fe emissions for two ensemble members each if the AERA is applied every five years starting in the

year 2025 for the 1.5°C target (**a-f, m-r**) and the 2.0°C target (**g-l, s-x**). The lines show realizations for different maximum lengths of the prescribed polynomial function in the AERA algorithm: fixed maximum length at 30 years (orange), fixed maximum length at 250 years (blue), and dynamical maximum length (green) as described in the methods. The shaded area shows the range of all configurations that fall within the likely range of ECS as defined by Sherwood et al. (2020)¹⁷. The grey shading in (**a**) indicates the uncertainty with which the anthropogenic warming can be determined ($\pm 0.2^\circ\text{C}$)⁵³⁻⁵⁶.

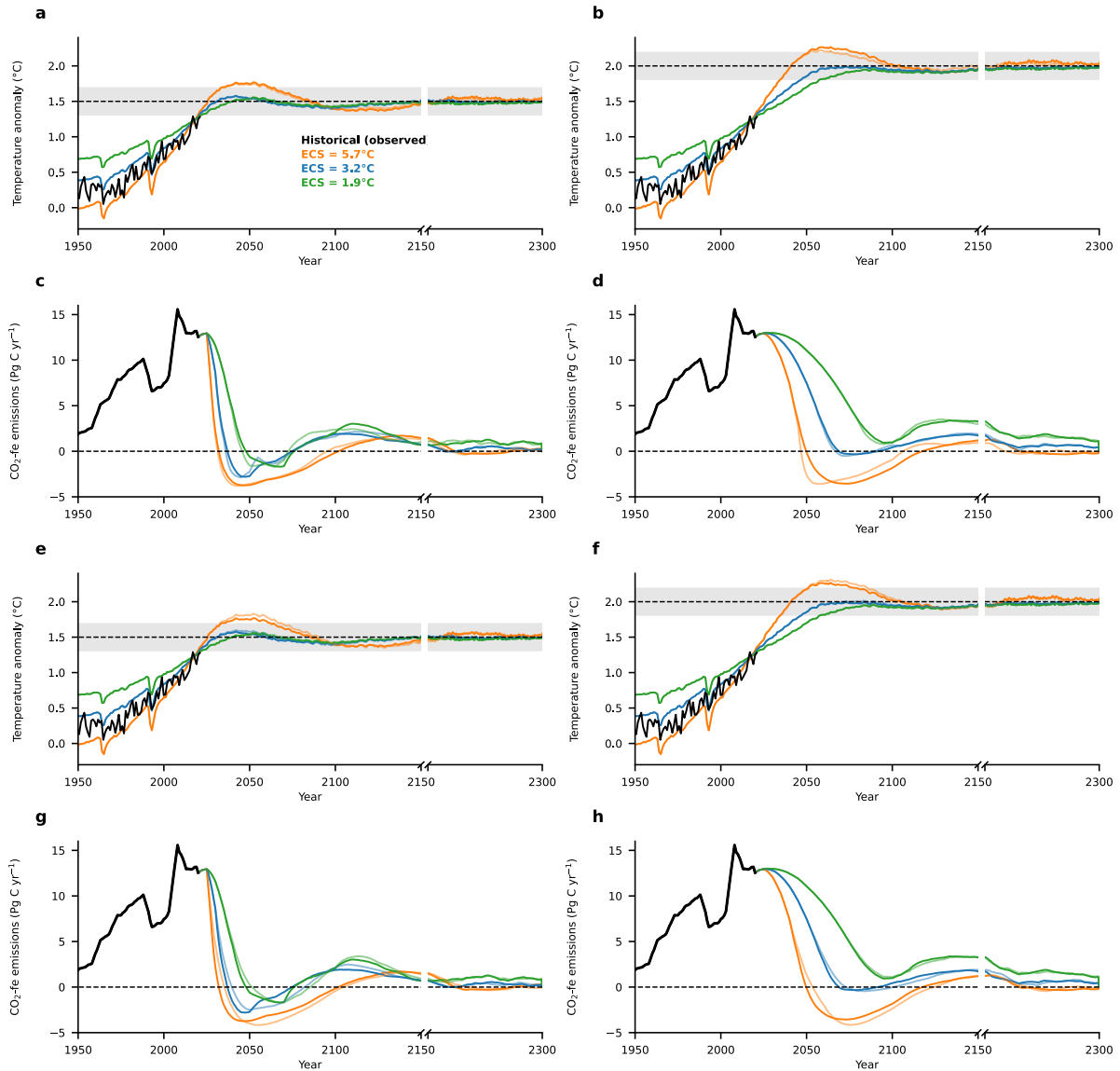


Supplementary Figure 2. Schematic of the implementation of the reduced atmospheric chemistry model. The reduced form atmospheric chemistry model is used to project non-CO₂ GHG concentrations and non-CO₂ (effective) radiative forcing from emissions of CO₂, CH₄, and N₂O, and of the precursors CO, VOC, and NO_x. Here, radiative forcing from aerosols and from halogens is prescribed (see methods). When using the CO₂-fe approach to calculate CO₂ equivalent emissions (left), radiative forcing from all non-CO₂ agents considered is added to yield total non-CO₂ radiative forcing, which is converted to CO₂-fe emissions (Smith et al., 2021). When using the GWP-100 approach to calculate CO₂ equivalent emissions (right), CH₄ and N₂O emissions are transferred to CO₂ equivalent

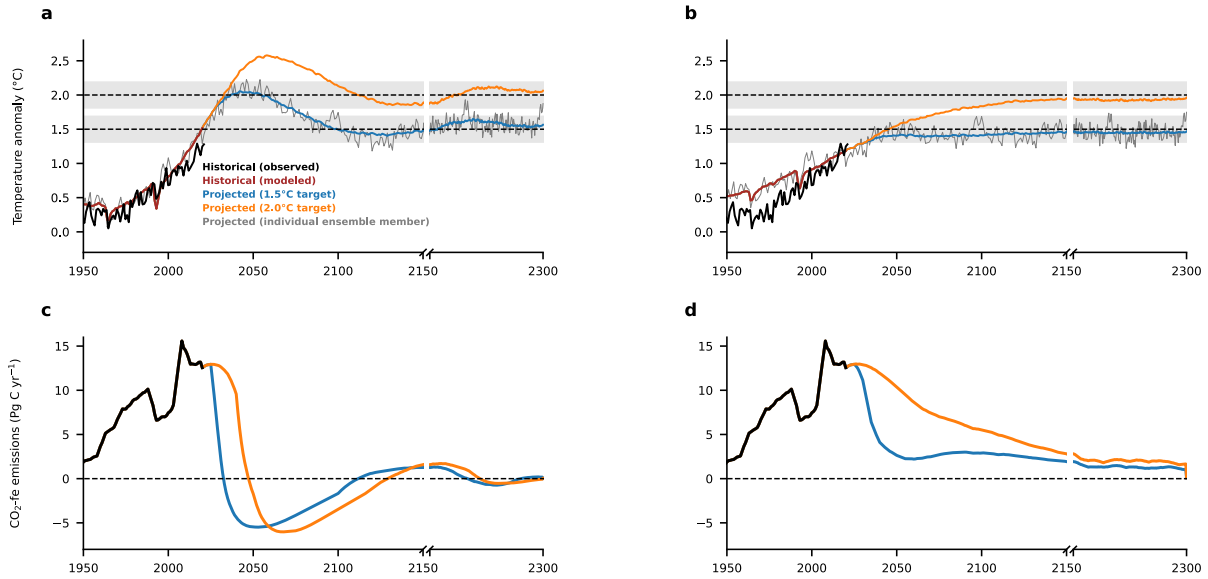
emissions using GWP-100, while radiative forcing from all remaining non-CO₂ agents considered is added to yield the remaining non-CO₂ radiative forcing, which is converted to CO₂-fe emissions. Projected non-CO₂ radiative forcing (together with fossil CO₂ emissions, and land use) is prescribed to the Bern3D-LPX model to project CO₂ concentration and global warming. In the standard simulations in this manuscript, the CH₄, N₂O, CO, NO_x, and VOC emissions evolve proportional to the CO₂ emissions in every year and the effective radiative forcing of aerosols and halogens are prescribed. In each year, the CO₂ emissions are chosen for which the resulting CO₂-fe emissions fit the prescribed CO₂-fe emissions by the AERA for that respective year.



Supplementary Figure 3. Adaptive emissions and resulting temperature anomaly for 1.5°C and 2.0°C target with varying allowed difference to the remaining emission budget. Temperature from 2020 to 2300 for three model configurations with varying ECS (orange = 5.7°C, blue = 3.2°C, and green = 1.9°C) averaged over four simulations each with different inter-annual variability for the (a, e) 1.5°C and (b, f) 2.0°C temperature target and (c, d, g, h) the respective CO₂-fe emission curves with the difference to the remaining emission budget (ξ) being (a-d) 2.5 Pg C (half of standard version) and (e-h) 10 Pg C. Temperature and emission curves are also shown for the standard version ($\xi = 5$ Pg C) (colored transparent lines). The grey shading in (a, b, e, i) indicates the uncertainty with which the anthropogenic warming can be determined ($\pm 0.2^\circ\text{C}$)^{53–56}.



Supplementary Figure 4. Adaptive emissions and resulting temperature anomaly for 1.5°C and 2.0°C target with varying allowed exceedance emissions. Temperature from 2020 to 2300 for three model configurations with varying ECS (orange = 5.7°C, blue = 3.2°C, and green = 1.9°C) averaged over four simulations each with different inter-annual variability for the **(a, e)** 1.5°C and **(b, f)** 2.0°C temperature target and **(c, d, g, h)** the respective CO₂-fe emission curves with the allowed exceedance emissions (ϵ) being **(a-d)** 5 Pg C (half of standard version) and **(e-h)** 20 Pg C. Temperature and emission curves are also shown for the standard version ($\epsilon = 10$ Pg C) (colored transparent lines). The grey shading in **(a, b, e, i)** indicates the uncertainty with which the anthropogenic warming can be determined ($\pm 0.2^\circ\text{C}$)^{53–56}.



Supplementary Figure 5. Adaptive emissions and resulting temperature anomaly for 1.5°C and 2.0°C target when the radiative forcing from aerosols is different than estimated. (a, b) temperatures and (c, d) associated CO₂-fe emissions averaged over four simulations each with different inter-annual variability (a, c) with ECS=5.7 and 40% increased simulated radiative forcing from aerosols and (b, d) with ECS=1.9 and 40% reduced simulated radiative forcing from aerosols. In each case, the AERA input for the radiative forcing from aerosols was not changed. Temperature observations based HadCRUT5 GMST time series are shown in comparison for the historical period.

References – Supplementary Information

91. Hurtt, G. C. *et al.* Harmonization of global land use change and management for the period 850–2100 (LUH2) for CMIP6. *Geosci Model Dev* **13**, 5425–5464 (2020).
92. van der Werf, G. R. *et al.* Interannual variability in global biomass burning emissions from 1997 to 2004. *Atmos Chem Phys* **6**, 3423–3441 (2006).
93. Riahi, K. *et al.* The Shared Socioeconomic Pathways and their energy, land use, and greenhouse gas emissions implications: An overview. *Global Environmental Change* **42**, 153–168 (2017).
94. van Vuuren, D. P. *et al.* Energy, land-use and greenhouse gas emissions trajectories under a green growth paradigm. *Global Environmental Change* **42**, 237–250 (2017).
95. le Quéré, C. *et al.* Fossil CO₂ emissions in the post-COVID-19 era. *Nat Clim Chang* **11**, 197–199 (2021).
96. Forster, P. *et al.* The Earth’s Energy Budget, Climate Feedbacks, and Climate Sensitivity. *Climate Change 2021: The Physical Science Basis. Contribution of Working Group I to the Sixth Assessment Report of the Intergovernmental Panel on Climate Change* Preprint at (2021).
97. Drew Shindell *et al.* The role of anthropogenic methane emissions in bridging the emissions gap. in *Emissions Gap Report 2021: The Heat Is On* (2021).
98. Naik, V. *et al.* Short-Lived Climate Forcers. *Climate Change 2021: The Physical Science Basis. Contribution of Working Group I to the Sixth Assessment Report of the Intergovernmental Panel on Climate Change* Preprint at (2021).
99. Canadell, J. G. *et al.* Global Carbon and other Biogeochemical Cycles and Feedbacks. *Climate Change 2021: The Physical Science Basis. Contribution of Working Group I to the Sixth Assessment Report of the Intergovernmental Panel on Climate Change* Preprint at (2021).
100. Prather, M. J., Holmes, C. D. & Hsu, J. Reactive greenhouse gas scenarios: Systematic exploration of uncertainties and the role of atmospheric chemistry. *Geophys Res Lett* **39**, (2012).